Aus der Klinik und Poliklinik für Radiologie
Klinik der Universität München
Direktor: Prof. Dr. Jens Ricke

Tumor-infiltrating lymphocytes as biomarkers to monitor local ablation of primary and secondary liver cancer

Dissertation
zum Erwerb des Doktorgrades der Medizin
an der Medizinischen Fakultät der
Ludwig-Maximilians-Universität zu München

vorgelegt von
Sijing Gu

aus
Yixing, China

2023

Mit Genehmigung der Medizinischen Fakultät

der Universität München

Berichterstatter:	Prof. Dr. Clemens C. Cyran
Mitberichterstatter:	PD Dr. Farkhad Manapov
	Prof. Dr. Dierk Vorwerk
Mitbetreuung durch den promovierten Mitarbeiter:	Dr. Marianna Alunni-Fabbroni
Dekan:	Prof. Dr. med. Thomas Gudermann
Tag der mündlichen Prüfung:	16.02.2023

Table of Content

List of figures

List of Tables

List of Abbreviations

AE	Abscopal effect
APCs	Antigen presenting cells
Bat3	HLA-B-Associated Transcript 3
Bregs	Regulatory B cells
CD	Cluster of differentiation
CRCLM	Colorectal cancer liver metastases
CT^1	Computed tomography
CT^2	Center of tumor
CTL	Cytotoxic T cells
CTLA-4	Cytotoxic T lymphocyte-associated protein 4
DAMPs	Damage-associated molecular pattern molecules
DAPI	4′,6-diamidino-2-phenylindole
EDTA	Ethylenediaminetetraacetic acid
FFPE	Formalin fixed and paraffin embedded
Foxp3	Forkhead box P3
HBV	Hepatitis B virus
HCC	Hepatocellular carcinoma
HCV	Hepatitis C virus
HDR	High dose rate
HDRBT	High-dose-rate brachytherapy
HRP	Horseradish peroxidase
HSC	Hepatic stellate cells
LAG3	Lymphocyte activation gene 3 protein
IHC	Immunohistochemistry
IL	Interleukin
IM	Invasive margin
LSEC	Liver sinusoidal endothelial cells
MDSCs	Myeloid-derived suppressor cells
MHC	Major histocompatibility complex
MIT	Micro-interventional therapy
MRI	Magnetic resonance imaging
NK cells	Natural Killer Cells

NR	Non-responder
OS	Overall survival
PD-L1	Programmed death ligand 1
PD-1	Programmed cell death protein 1
PFS	Progression free survival
RE	Radioembolization
ROI	Region of interest
RECIST	Response Evaluation Criteria in Solid Tumors
RT[1]	Radiotherapy
RT[2]	Room temperature
SD	Standard deviation
SIRT	Selective internal radiation therapy
SPSS	Statistical Product and Service Solutions
SR	Sustained responder
TAMs	Tumor-associated macrophages
TB	T and B cell
TBS	Tris-buffered saline
TBS-T	Tris-buffered saline with Tween 20
TCR	T-cell receptor
TGF-β	Transforming growth factor beta
TIGIT	T cell immunoreceptor with Ig and ITIM domain
Th	T helper cells
Tc	T cytotoxic cells
TILs	Tumor infiltrating lymphocytes
Tim3	T cell immunoglobulin and mucin domain-containing protein-3
TME	Tumor microenvironment
TR	Transient responder
Y90	Yttrium 90

1. Introduction

1.1. Liver cancer

Among all the types of tumor, liver cancer is the fifth most common and one of the major causes of death (1). Hepatocellular carcinoma (HCC) is the most prevalent primary liver cancer with a growing incidence rate worldwide, accounting for approximately 75% of all cases (2-4). The major risk factors for HCC development are genetic background, HBV/HCV induced hepatitis, obesity, alcohol abuse, non-insulin-dependent diabetes, and non-alcoholic fatty liver diseases (5, 6). The liver is also a common site for distal metastases derived from colorectal, breast, cervical, and prostate cancer (7-10). Although different options are available for clinical management of hepatic malignancies, treatment is often complexed by a series of elements, such as the tumor size, the clinical stage of the cancer, the patient age and general health, the location of blood vessels (11). Liver transplant and surgery are regarded as the best treatment options with a 5-year survival rate of over 50% (12). However, surgical resection or transplant are suitable for only fewer than 20% of patients diagnosed with liver cancer since the majority are already at an advanced stage of the disease by the time the symptoms are shown (13). For those patients not eligible for curative measures, alternative treatments, including radiation therapy, chemotherapy and targeted therapy, are still an option. Radiotherapy, or radiation therapy (RT), has become one of the leading treatment methods for unresectable liver cancer patients (14, 15). RT, including radioembolization and brachytherapy, involves the implementation of radioactive microspheres or X-rays targeted to liver lesions, inducing damage of cellular DNA and selective death of cancer cells (16). RT is mostly a local, targeted treatment, thereby minimizing the damage of surrounding normal liver tissue (17).

1.2 Brachytherapy and Yttrium-90 (Y^{90})-radioembolisation (RE)

Brachytherapy is a widely used RT modality characterized by a high safety profile and minimal invasiveness. In particular, image-guided interstitial high-dose-rate brachytherapy (HDRBT) was introduced by Ricke *et al.* into a clinical setting (18, 19). To destroy the tumor, the source of radiation is temporarily placed inside or near the targeted lesion via radioactive implants (20). The entire procedure is guided through

advanced imaging methods such as MRI or CT scan. HDRBT delivers radiation at a high dose directly to the target lesion in a single fraction while protecting adjacent healthy tissues from exposure (21).

Radioembolization (RE), also known as selective internal radiation therapy (SIRT), is a type of brachytherapy, where Yttrium-90 (^{90}Y)-coated microspheres are injected under image guidance by a transarterial catheter in the hepatic arteries (22). The mechanism underlying this technical practice is that, while the portal vein supplies normal liver parenchyma, liver tumors are preferentially fed by arterial blood vessels (23, 24). Once they have reached the target lesion, the blood supply is blocked by the isotope-loaded particles, while the radioactive isotope releases a high dose of radiation directly in the lesion, sparing the adjacent healthy liver tissue (25). A schematic description of the technical modalities characterizing brachytherapy and radioembolization is provided in figure 1.

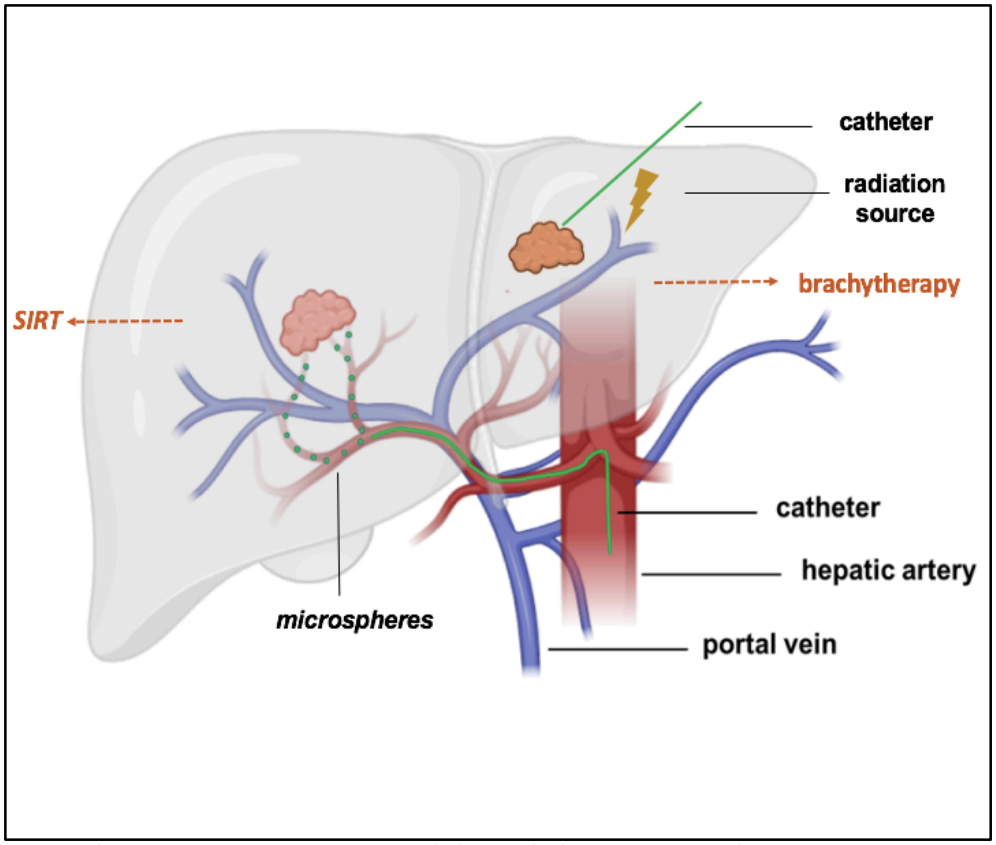

Figure 1. Schematic representation of SIRT (left hepatic lobe) and brachytherapy (right hepatic lobe). In the circumstance of SIRT, ^{90}Y isotope encapsulated by microspheres is injected under imaging guidance through a transarterial catheter. The specific liver artery only supplying the tumor is blocked, therefore minimizing the damage to the nearby healthy tissues. In the case of brachytherapy, the radioactive source, releasing high doses of radiation to the targeted lesion, is directly applied to the tumor.

Not only has RT proven to alleviate symptoms and improve the quality of patients' lives (26), it has also demonstrated antitumor efficacy by downsizing the lesion, slowing tumor progression (23, 27), and prolonging overall survival (28, 29). In comparison to other palliative treatments, the most attractive advantages of RT are higher efficacy, fewer side effects, and better safety over time (30, 31). In particular, the invasiveness of RT is minimal as no surgical incision is necessary (26). For this reason, in advanced metastatic malignancies, RT and especially brachytherapy can be combined with other second-line treatments, such as chemotherapy or used as a neoadjuvant therapy prior to surgery, thus enhancing the patient response to therapy (32). Despite a lower complication rate and a high technical success and, long-term benefits of RT are still damped by the relapse of local and distal lesions. This is largely contributed by either the incomplete tumor ablation or technical limitations in phase of dose delivery (33, 34). Therefore, the reduction of recurrence, especially in the distant site, currently remains a clinical challenge.

1.3 Abscopal effect

The word "abscopal" derives from the Latin "*ab scopus*", which means "away from the target". Abscopal effect refers therefore to a secondary effect induced by RT on distal, not yet treated lesions. In particular, ionizing radiation can induce an indirect immune response in the non-irradiated site, leading to a size reduction of the untreated lesions. In this case, the effect is defined as positive abscopal effect (AE). Biologically, AE is based on an immune-mediated response triggered by RT (figure 2A) (35). The antigens released by the irradiated tumor cells induce the activation of the antigen-presenting cells (APCs), boost the recruitment of tumor-infiltrating lymphocytes (TILs) and promote the secretion of immune-stimulatory chemokines, functioning as an *in situ* vaccine against the untreated lesion (36, 37). However, AE induced solely by RT is a very rare event (38, 39) and it is usually limited only to a few types of malignancy, such as HCC (40), melanoma (41) and breast cancer (42). AE is frequently repressed by the presence of a highly immunosuppressive tumor microenvironment (TME), mostly infiltrated by negative regulators, such as regulatory T cells, tumor-associated macrophages (TAMs) and myeloid-derived suppressor cells

(MDSC) (35, 43). These cells can weaken the inflammatory effects exerted by radiation and even inhibit the immune cells from targeting and eliminating tumor cells. In addition, as a consequence of radiation, damaged tissues release immune-inhibitory factors such as damage-associated molecular pattern molecules (DAMPs), the tumor growth factor (TGF-ß) and galectin-1 that together play a pro-tumorigenic effect, further suppressing T cell infiltration and activity (figure 2B) (44). As a consequence, these aforementioned negative regulators of AE, including immune-suppressive cell components and cytokines, cannot prevent the enlargement of the yet untreated lesions and potentially inhibit the occurrence of AE (figure 2C). In conclusion, the shift in the immune pattern induced by RT is able to define the direction of AE (43, 45, 46).

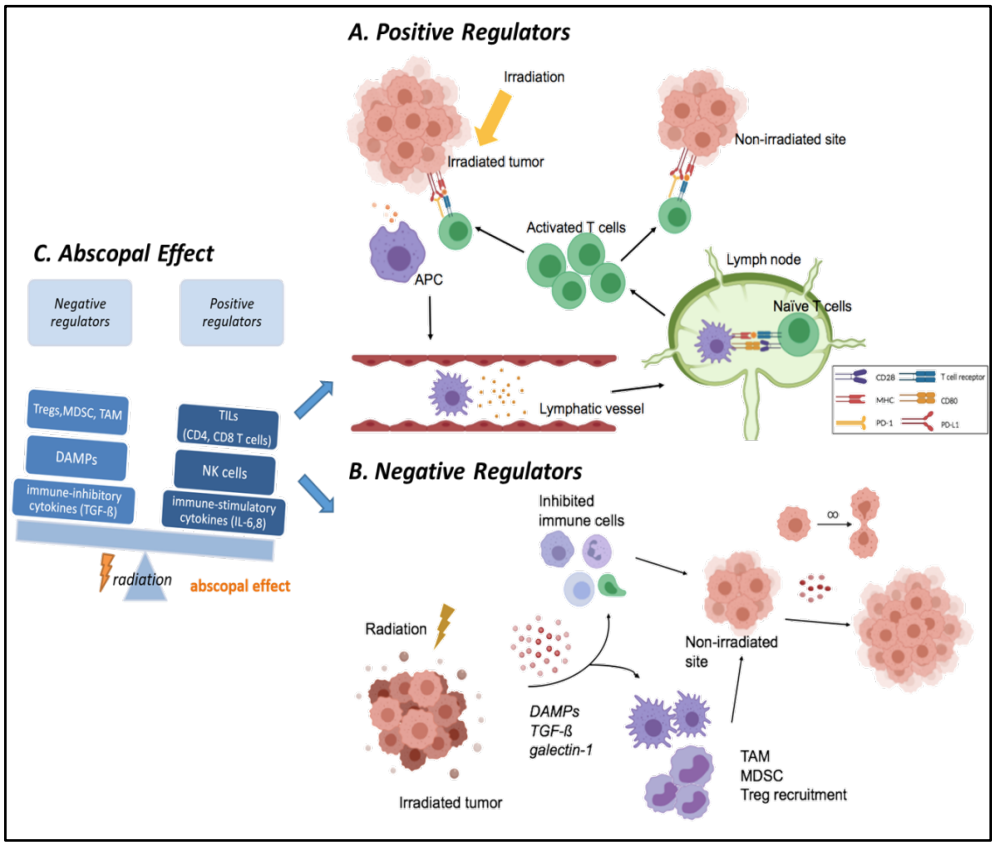

Figure 2. Possible mechanisms of RT-induced abscopal effect. (A) In the case of a positive abscopal effect, radiation induces the release of antigen from damaged tumor cells. Antigens are taken up by APCs and then travel to the lymph node. There, naïve T cells interact with APCs displaying antigens. As a result, primed and activated T cells can then recognize and target tumor cells in both the irradiated lesion and the non-irradiated distant site. (B) In the circumstance of massive existence of negative regulators, radiation destroys tumor cells and helps to elicit immune-suppressive cytokines (TGF-ß, galectin-1, etc), therefore dampening the activity of immune cells, promoting the recruitment of macrophages, MDSCs and Tregs as well as facilitating the growth of the tumor. (C) The interplay between positive and negative regulators modulates the direction of abscopal effect after radiation.

1.4 Tumor-infiltrating lymphocytes (TILs)

In humans, the immune response is driven by the innate and adaptive immunity, which work together as a cooperative system to eliminate foreign pathogens (47). In innate immunity, the clearance of a pathogen is conducted by non-specific defense mechanisms such as physical barriers, inflammatory processes and the complement system. In case the innate immunity is not able to target and eliminate the pathogen, , the adaptive immune system is therefore stimulated (48). In this case, the major cellular components of adaptive immunity, namely T and B lymphocytes, act against specific antigens carried by the pathogen, enabling a stronger and more targeted immune response (48, 49). Upon encounter of antigens, B cells progress towards differentiation into plasma cells and release antibodies which by binding to the specific antigen, contributes to clearance of the antigen from the host immune system. Furthermore, cytotoxic T cells (CTL) are activated to boost the elimination of corresponding antigens, while T helper cells, involved in both pathways, release related cytokines to facilitate both B cell and T cell-mediated immune response (48, 50) (Figure 3).

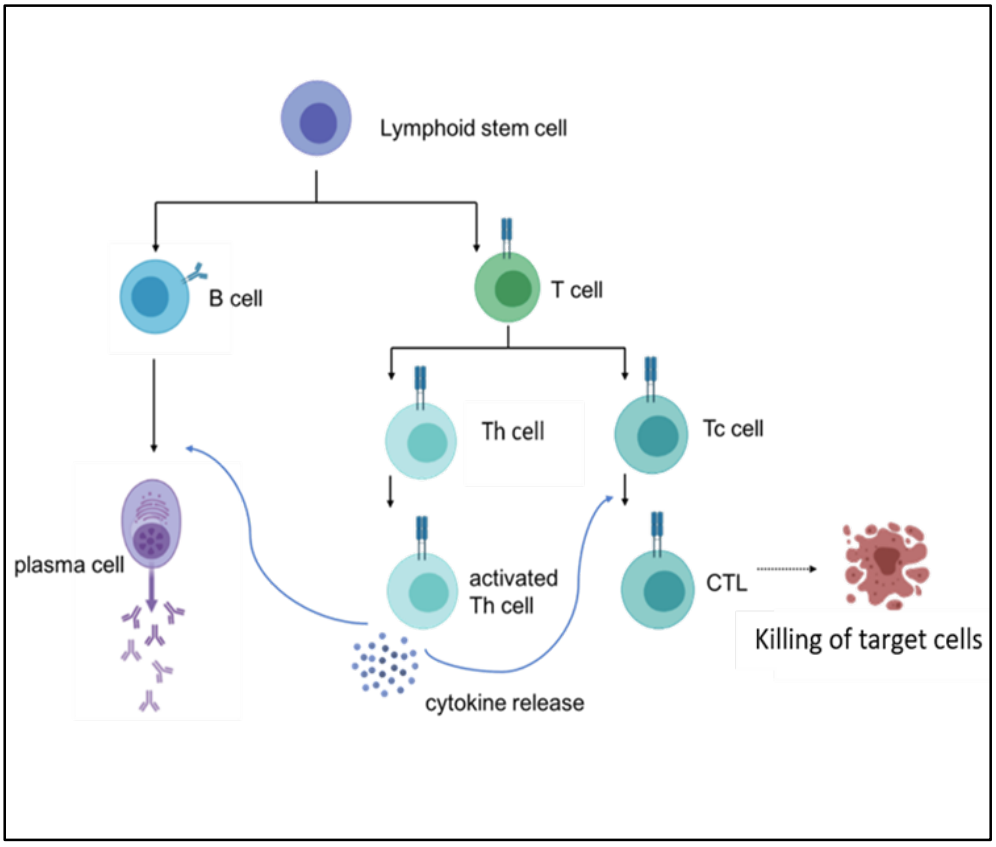

Figure 3. Overview of adaptive immunity. T and B lymphocytes are derived from lymphoid stem cells. After interaction with antigens, activated T helper cells (Th) release cytokines to boost the transition from T cytotoxic (Tc) cells to CTL. The differentiation of B cells to antibody-producing plasma cells is also promoted by activated T helper cells, which further mediates the clearance of antigens.

In cancer immunity, it is soundly proven that TILs play an irreplaceable role in the fight against cancer. Several studies have correlated TILs' activities to clinical prognosis in a variety of human cancer types (51-53), including liver metastasis (54). In particular, five subtypes of TILs including cytotoxic (CD8+)-, T helper (CD4+)-, regulatory (FOXP3+)- and memory (CD45+)-T cells and B (CD20+)- cells interact with tumor cells and their dynamic interplay within TME can influence the balance between a pro- and anti-tumor effect played by the immune system (55) (figure 4).

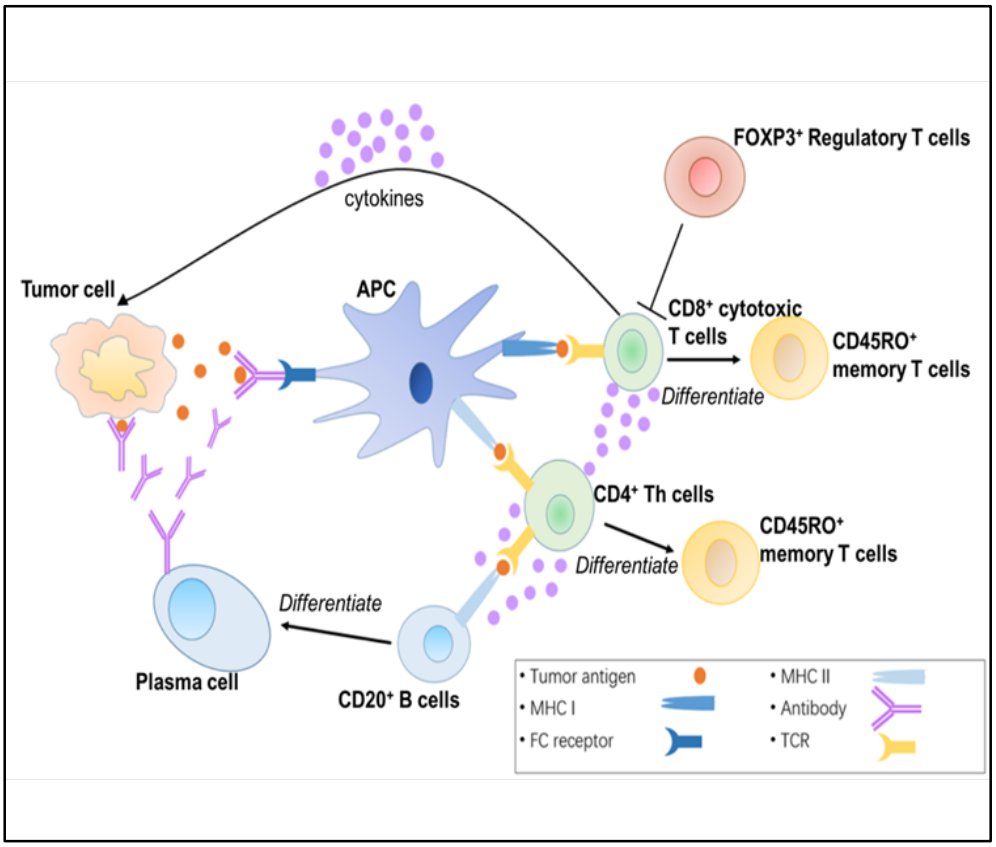

Figure 4. Illustration of the immune microenvironment. Physiologically, $CD8^+$ cytotoxic T cells, $CD4^+$ T helper cells, $CD20^+$ B cells, $CD45RO^+$ memory T cells and $FOXP3^+$ regulatory T cells are crucial players within the immune microenvironment. Tumor cells are eliminated either by the specific antibody secreted by plasma cells or directly through $CD8^+$ cytotoxic T cell-led pathway. Cancer cells are commonly attacked and eliminated through an intricate collaboration and interplay between the different types of immune cells.

Accumulating evidence also suggests that TILs are involved in the modulation of AE (56). Hence, the analysis of TILs in TME could shed light on the cellular and molecular mechanisms leading to RT-induced AE.

1.4.1 $CD4^+$ T helper cells

T helper (CD4+) cells are mainly involved in the adaptive immune response displaying the CD4 (cluster of differentiation 4) glycoprotein as a major surface receptor (57, 58). $CD4^+$ cells are activated through the interaction with the major histocompatibility complex (MHC) class II expressed on APC or B cells and are major regulators of the inflammatory process. They are crucial in modulating overall immune response against pathogens (59). Multiple studies have shown that $CD4^+$ cells have a pivotal effect in the immune reaction to cancer (57, 60). However, their biological activities heavily depend on the nature of TME and therefore their prognostic value is controversial. For example, in HCC (61) and pancreatic cancer (62, 63), $CD4^+$ cells activate $CD8^+$ cells through the secretion of cytokines. Therefore, they support an anti-tumor immune response and predict a favorable clinical outcome (64). On the contrary, in colorectal cancer liver metastasis (CRCLM), $CD4^+$ cells can impair the tumor-attacking function of CD8 cells; in this case, a high amount of $CD4^+$ cells in the lesions predicts a worse clinical outcome (65).

1.4.2 $CD8^+$ cytotoxic T cells (CTL)

Cytotoxic (CD8+) T cells are considered the most efficient fighters against cancer in adaptive immunity (66). These cells display the CD8 (cluster of differentiation 8) glycoprotein and are commonly activated by cytokines released from $CD4^+$ cells as well as by the interaction with antigens expressed on the surface of APC and associated with the tumor or directly with tumor cells (67, 68). $CD8^+$ cells induce the apoptosis of target cells through the FAS/FAS L pathway. In particular, the FAS ligand (FAS L), expressed on $CD8^+$ cells, binds to the receptor FAS on tumor cells, inducing cellular death (69). Additionally, $CD8^+$ cells promote the anti-tumor immunity by secreting immune-stimulatory cytokines, for example tumor necrosis factor α (TNF-α) and interferon γ (INF-γ). TNF-α and IFN-γ (70). Based on multiple studies, the importance of $CD8^+$ cells in cancer immunity has been largely proven. Growing evidence shows that a higher amount of $CD8^+$ cells in TME is associated with a better

therapy response and prolonged survival in various types of cancers, including metastatic colorectal, gastric, breast cancer and HCC, indicating a strong antitumor role played by $CD8^+$ cells in frame of the immune microenvironment (71-74).

1.4.3 $FOXP3^+$ regulatory T cells (Tregs)

Regulatory (FOXP3+) T cells represent a subpopulation of $CD4^+$ T cells expressing the transcription factor *Forkhead box P3* (FoxP3) (75). Tregs are involved in modulating the immune system, maintaining self-tolerance and preventing autoimmune diseases (76). In TME, Tregs act as immune-suppressive cells, inhibiting the anti-tumor activity of CD8 cells via the release of cytokines, for example TGF-β, IL-10 and IL-35 (77-79). As a consequence, Tregs contribute to progression of the primary tumor as well as development of distant metastases (80), and therefore can be associated with a poor prognosis in different types of cancers, including HCC (81-84). However, in other malignancies, such as in colorectal cancer, increased infiltration of Tregs in the tumor correlates to a better prognosis (85). Thus, the role of Tregs in cancer immunity is still not thoroughly clarified and remains controversial (75).

1.4.4 $CD45RO^+$ memory T cells

Memory (CD45+)-T cells are derived from naïve T cells. After antigen-induced activation, naïve T cells are then differentiated into memory T cells and effector T cells (86). While pathogens are killed and eradicated by effector T cells, after the first elimination of antigen, memory cells maintain in the host immune system preparing to initiate a stronger or more intense immune response once they re-encounter a same antigen (87). Research on numerous types of cancers, including HCC and CRC, indicates that patients with a higher infiltration level of $CD45RO^+$ cells tend to have an improved prognosis (88-94).

1.4.5 $CD20^+$ B cells

The majority of B cells extensively express a pan-B cell marker- CD20. B cells have multiple functions ranging from antibody production to antigen presentation and cytokine release (95, 96). Most importantly, B cells contribute largely to the antigen-specific immune response as precursors of plasma cells. After the interaction

with $CD4^+$ cells, they start to produce antibodies that, in the case of cancer, can directly target tumor cells present in the TME (97, 98). B cells also work as antigen-presenting cells in support of activated $CD8^+$ cells, thus further contributing to the elimination of malignant cells (99). Finally, B cells can promote anti-tumor immunity by targeting cancer cells directly through the secretion of immune-stimulatory cytokines such as granzyme B (100, 101). Despite a clear anti-tumor activity recognized to B cells, the prognostic value of B cells is still under debate (102). For example, in HCC (103), a high infiltration of B cells is correlated to favorable prognosis, while in breast cancer (104), B cells could instead promote tumor progression and have a negative effect on overall survival. Therefore, the clinical relevance of B cells remains uncertain and needs to be further explored.

1.5 Immune exhaustion and immune regulators

In chronic infections or tumor microenvironment, immune response can also be potentially impaired and therefore the immune system fails to work as intended. In this regard, immune exhaustion, known as a dysfunctional state of T cells, has been recently highly noted (105). In adaptive immunity, naïve T cells are differentiated into short-lived effector T cells, which are rapidly deactivated after the peak of immune response (106). This kind of homeostasis, aiming to maintain immune tolerance, is mostly modulated through expression on the T cell surface of specific inhibitory receptors called immune checkpoints such as cytotoxic T lymphocyte-associated protein 4 (CTLA-4), programmed death ligand 1 (PD-1), programmed cell death protein 1 (PD-L1), and T cell immunoglobulin and mucin domain-containing protein-3 (Tim3). These proteins act as natural brakes of T cells, keeping them inactive and therefore downregulating the immune response (107, 108). In the TME, the initiation of immune exhaustion is also triggered by the persistent exposure of T cells to tumor-associated antigens, inducing the higher expression of immune inhibitory receptors on T cells. As a result, dysfunction or even death of T cells can take place, impairing their anti-tumor immunity (109, 110). Immune checkpoint inhibitors are widely used clinically as a powerful strategy to interrupt immune exhaustion and reinvigorate the functionality of T cells (111, 112).

PD-L1 is expressed broadly on immune cells, such as T and B cells, and antigen-presenting cells, whereas PD-1 is mainly expressed on T and B cells (113, 114). In physiological conditions, the binding of PD-L1 and PD-1 induces a decreased proliferation of T cells, ultimately suppressing the over-activation of the immune system and preventing autoimmune diseases (115, 116). However, in TME, tumor cells can overexpress PD-L1 as a mechanism to escape the immune response (114, 117). By binding to the PD-1 receptor expressed by T cells via PD-L1, cancer cells are able to deactivate or even exhaust T cells (118, 119), therefore hampering the anti-tumor activity in the immune system (120). Studies have shown that PD-1 and PD-L1 are highly expressed in a wide range of tumor types (114, 117). Additionally, the expression level of PD-L1 or PD-1 has a mostly negative association with overall survival of patients (121, 122) (figure 5A).

T cell immunoglobulin and mucin domain-containing protein-3 (Tim3) is ordinarily identified as a receptor expressed on effector T cells, as well as other types of cells, for example macrophages and NK cells (123). In normal physiology, HLA-B-Associated Transcript 3 (Bat3), a negative regulator, binds to Tim3 to form a stable complex on the membrane of T cells, therefore preserving the function of activated T cells and averting its exhaustion. In TME, galectin9, a receptor of Tim3, is expressed by tumor cells. The binding of galectin 9 to Tim3 induces the release of Bat3 from Tim3, with consequent exhaustion of T cells and inactivation of the immune response (124). The expression of Tim-3 has been detected in various tumor entities (123, 125, 126). Several independent studies have also demonstrated that in TME, high expression levels of Tim3 accelerate the dysfunction or exhaustion of T cells; thus, correlating to a poorer overall survival rate (127, 128)(Figure 5B).

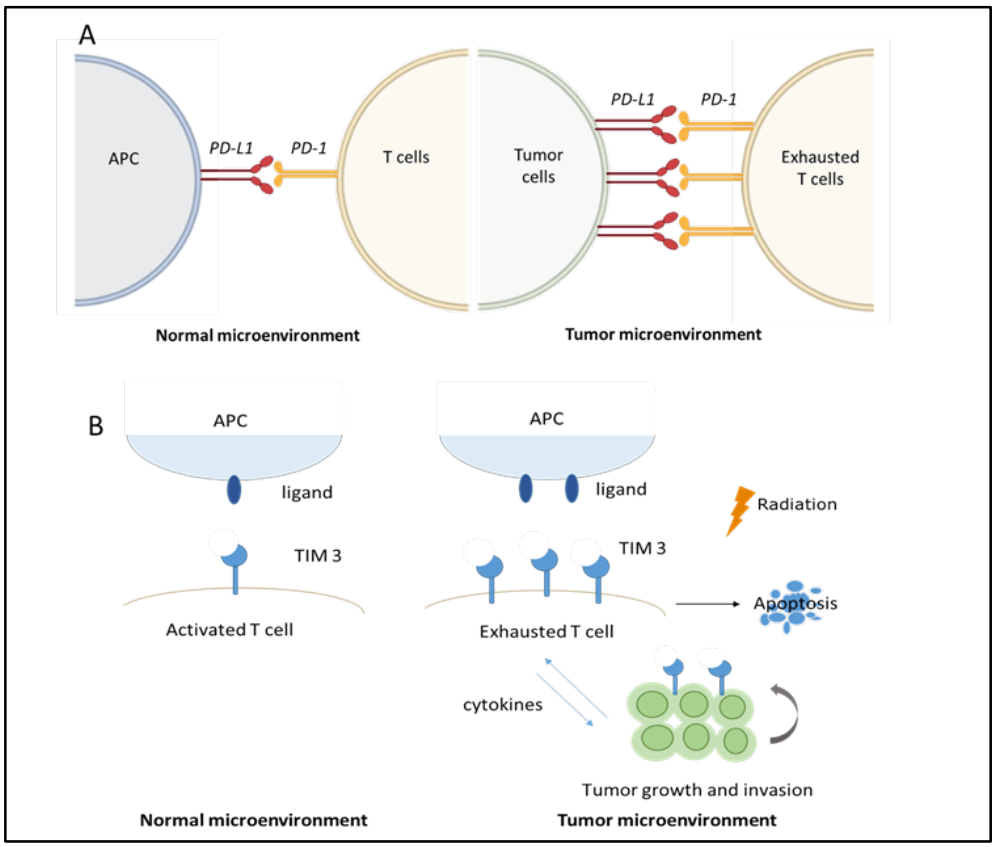

Figure 5. Role of PD-1/PD-L1 pathway and Tim3. (A) In healthy microenvironments, inhibitory receptors, such as PD-1, on activated T cells, interact with its ligand PD-L1 present on APC. The binding of PD-L1 and PD-1 leads to the suppressed function of T cells, thus suppressing the over-activation of the immune response and maintaining a self-tolerance. In TME, PD-L1 expressed by tumor cells binds to PD-1 on T cells, inducing the exhaustion and the apoptosis of T cells and preventing tumors from being eliminated. (B) In healthy conditions, Tim3 on activated T cells binds to its ligand on APC in order to maintain homeostasis. In TME, Tim3 is over-expressed on T cells, resulting in T cell exhaustion and apoptosis. Meanwhile, the cytokines released by exhausted T cells promote growth and invasion of tumors, which in return exacerbate further impairment or exhaustion of T cells.

1.6 TILs as biomarkers for liver cancer

Despite the impressive progress made in cancer treatment based on RT, the recurrence rate in distant, untreated sites remains high and the prognosis poor. Nevertheless, under certain circumstances, a positive abscopal effect is likely to be induced after radiotherapy, with the regression of the distal, yet not treated lesions. The mechanism behind this systemic effect of RT is still poorly understood (38). However, mounting evidence suggests that TME and TILs could be at least in part involved in modulating the abscopal effect induced by RT (129).

Although helpful in most clinical cases, the tumor-node-metastasis (AJCC/UICC-TNM) clinical classification system has a limited predictive value and fails to anticipate potential benefits of the therapy patients receive (130). Therefore, a robust evaluation system for better stratification of patients and early prediction of clinical outcome is still required. Recent studies have raised interest into the investigation of the "immune contexture", as found in the TME (75). It has been reported that immunoscores based on TILs' relative ratios can offer more precise information on therapy response and clinical outcome (94, 131). While immunoscores based on single markers do not fully reflect the immune landscape and have a limited prognostic role (132, 133), immunoscores based on the ratio between two different markers (for example CD8/CD3, CD8/CD4 and CD8/FoxP3) have been shown to better and more comprehensively define the immune contexture and to become stronger prognostic markers. For example, Galon *et al*. showed that an immunoscore based on a CD8/CD3 T cells ratio (CD3 being a receptor expressed on all mature T cells) is a favorable predictor of clinical outcome in CRC (132, 134). Similarly, others have shown that a high CD8/FoxP3 ratio is correlated to a better clinical outcome in CRCLM and rectal cancer (135, 136). However, immunoscores do not always provide clear information and sometimes lead to conflicting results, probably due to different features and components of TME. One example can be given by the CD8/CD4 ratio in CRCLM, where different groups found contradictory results (65, 137). Until now, the predictive and prognostic value of immunoscores in liver metastasis has not yet been fully clarified. Therefore, our study intends to address this gap in knowledge.

1.7 Main hypothesis and objective of the study

The hypothesis of this study was that RT treatment of hepatic lesions has an indirect effect on the composition and distribution of TILs in adjacent, not yet treated lesions, therefore influencing patient response to therapy.

The evaluation of the predictive and prognostic significance of TILs in liver metastases and in HCC was the main goal of the present study. The examined immune panel included cytotoxic (CD8+)-, T helper (CD4+)-, regulatory (FOXP3+)- and memory (CD45+)-T cells and B (CD20+)- cells. Changes in TILs composition, density and spatial distribution were evaluated in separate lesions receiving sequential therapy sessions. Therefore, the immune profile we established, which is composed of the aforementioned five subtypes of TILs, could have the potential to predict the occurrence of an abscopal effect providing early information in terms of patients' clinical outcome.

The ultimate goal of the study was to contribute to the optimization of radiological treatment regimens in liver cancer patients based on individualized immune profiles, providing a more precise stratification of the patients and therefore offering personalized oncological therapies in combination with other adjuvant treatments when necessary.

2. Materials and Methods

2.1 Material

2.1.1 Instrumentation

Autoclave/ VX-95	Systec, Nuremberg, Germany
Computer& monitor for microscope/ -Cooler Master TEAC	Leica, Wetzlar, Germany
Microtome/Leica RM 2245	Leica, Wetzlar, Germany
Microscope/ Leica DM 2500 DM IL LED	Leica, Wetzlar, Germany
Microwave/ HF24M541	Siemens, Munich, Germany
Micro-centrifuge/ 5418 R	Eppendorf, Hamburg, Germany
Oven/INE 500 (Model 100-800)	Memmert, Schwabach, Germany
pH-meter/ Material No.: 30266658	Mettler Toledo, Columbus, OH
Pipettes/Research Plus®	Eppendorf, Hamburg, Germany
Quantitative Pathology Imaging System	AKOYA Biosciences, Marlborough, MA
Vectra Polaris™ Automated	AKOYA Biosciences, Marlborough, MA
Vortex/ G560E	Benchmark, NYC, NY
Water bath/ WNB 14	Memmert, Schwabach, Germany
Water bath for microtome/ GFL 1052	GFL, Burgwedel, Germany

2.1.2 Chemicals and Reagents

10% buffered formalin	SIGMA, St. Louis, MO
20X Citrate buffer, pH 6.0	Life Technologies, Waltham, MA
DAB (3-3'- Diaminobenzidine) - staining	Cell Signaling Technology, Danvers, MA
DAB (3-3'- Diaminobenzidine) - staining	Dako, Santa Clara, CA
99.8% Ethanol	Carl Roth, Karlsruhe, Germany
96% Ethanol	Carl Roth, Karlsruhe, Germany
70% Ethanol	Carl Roth, Karlsruhe, Germany
Eosin-G	Carl Roth, Karlsruhe, Germany
32% Hydrochloric Acid	Applichem GmbH, Darmstadt, Germany
30% Hydrogen peroxide	Carl Roth, Karlsruhe, Germany
Mayer's hemalum	Merck KGaA, Darmstadt, Germany
Mounting Medium (Neo-mount)	Merck KGaA, Darmstadt, Germany

Normal Goat Serum	Cell Signaling Technology, Danvers, MA
Neoclear	Merck KGaA, Darmstadt, Germany
Opal 7 ™ Tumor Infiltrating Lymphocyte Kit	Akoya Bioscience, Marlborough, MA
10X SignalStain® EDTA Unmasking Solution	Cell Signaling Technology, Danvers, MA
Sodium chloride	Applichem GmbH, Darmstadt, Germany
Trizma Base	SIGMA, St. Louis, MO
Tween-20	Bio Rad Laboratories, Hercules, CA

2.1.3 Consumables

Centrifuge falcon (15mL)	SARSTEDT, Nümbrecht, Germany
Cover slips	Thermo Fisher Scientific, Waltham, MA
Superfrost microscope slides	Thermo Fisher Scientific, Waltham, MA
Parafilm	Bemis, Neenah, WI
Pipette tips	Eppendorf, Hamburg, Germany
Reaction tubes (1mL)	Eppendorf, Hamburg, Germany
Vectashield Mounting Medium	BIOZOL, Eching, Germany

2.1.4 Buffers and Solutions

1x AR9/AR6 retrieval buffer	90 ml dH_2O
	10 ml 10x AR9/AR6 retrieval buffer
3% hydrogen peroxide	900 ml dH_2O
	100 ml 30% Hydrogen Peroxide
10x TBS buffer (pH 7.5)	91g Sodium chloride
	60g Trizma Base
	1L dH_20
1x TBST buffer	1800 ml dH_2O
	200 ml 10x TBS buffer
	2 ml Tween-20
4% buffered formalin	300 ml dH2O
	200 ml 10% buffered formalin
Blocking Solution	500 µl Normal Goat Serum
	10 ml 1X TBST
1x Citrate buffer	190 ml dH2O

	10 ml Citrate buffer (20X) pH 6.0
DAPI solution	2 ml 1x TTBS
	4 drops DAPI stock solution
1x EDTA unmasking solution	180 ml dH_2O
	20ml SignalStain® EDTA Unmasking Solution (10X)
Opal Fluorochrome stock solution	100 µl 1x Amplification Diluent
	2 µl Opal fluorochrome

2.1.5 Antibodies

Staining kit (*CD4,CD8,CD20,FoxP3,CD45RO*)	Akoya Bioscience, Marlborough, MA
PD-L1 (E1L3N) XP (rabbit mAb)	Cell Signaling Technology, Danvers, MA
PD-1 (NAT105) (mouse mAb)	Abcam, Cambridge, UK
Tim3 (EPR22241) (rabbit mAb)	Abcam, Cambridge, UK

2.1.6 Software

Vectra Polaris	AKOYA Biosciences, Marlborough, MA
Phenochart™	AKOYA Biosciences, Marlborough, MA
inForm ®	AKOYA Biosciences, Marlborough, MA
Image J	NIH, Bethesda, MD
SPSS Statistics Version 21.0.0	IBM, New York, NY
https://biorender.com	Biorender, Toronto, Canada

2.2 Methods

2.2.1 Preparation of paraffin sections

Biopsies collected from target lesions were fixed in 10% formalin and shipped to the Department of Pathology (LMU Klinikum, Munich, Germany) for tissue processing and paraffin embedding. Cold paraffin blocks were cut at desired thickness (1.5 µm) on a microtome, placed in a preheated (42 °C) water bath for a few seconds before drawing them onto the surface of Superfrost microscope slides. Slides were dehydrated at 20°C overnight and preserved at 4°C for further use.

2.2.2 Hematoxylin and Eosin staining (H&E staining)

Paraffin sections were dried overnight at 55°C, then deparaffinized and rehydrated according to standard procedure (3 times for 10 minutes in xylene substitute Neo-Clear, 2 times for 5 minutes in 100% ethanol, 1 time of 3 minutes each in 96%, 90%, 80% and 70% ethanol and 2 times for 5 minutes in distilled water), followed by nuclear staining in Mayer's hemalum solution for 5 minutes. Finally slides were rinsed in distilled water, followed by a last washing step in running water for 10 minutes. For cytoplasmic staining, slides were incubated in Eosin-G for 2 minutes, rinsed with tap water and incubated briefly in 80% ethanol for differentiating. After dehydrating the specimens in a graded series of ethanol and Neo-Clear (1 time of 30 seconds each in 90% and 96% ethanol, 2 times for 5 minutes in 100% ethanol, 2 times for 5 minutes in Neo-Clear), slides were covered with Neo Mount embedding medium and then microscopically examined at 40x magnification by two independent reviewers.

2.2.3 Immunophenotyping

Paraffin sections were dried overnight at 55°C, then deparaffinized and rehydrated according to standard procedure (2 times for 15 minutes in 100% xylene, 1 time of 5 minutes each in 100%, 96 %, 70% ethanol and distilled water), followed by fixation in 4% buffered formalin solution at RT for 20 minutes. For heat-induced antigen retrieval, slides were cooked in a specific antigen retrieval buffer (AR6 or AR9) for 15 minutes at 96°C, let to cool for 15 minutes at RT, rinsed in 1x TTBS buffer 3 times for 2 minutes. For each antibody (anti- CD4, -CD8, -CD20, -FoXP3 and –CD45RO), a complete cycle including blocking (10 minutes at RT), primary antibody incubation (1 hour at RT), secondary antibody incubation (10 minutes

at RT), Opal Fluorochrome incubation (Opal 520-CD4, Opal 570-CD8, Opal 540-CD20, Opal 620-FoxP3 or Opal 650-CD45RO for 10 minutes at RT) and antigen removal (15 minutes at 96°C) was performed (table 1 and figure 10). In between the steps, slides were washed 3 times in 1xTTBS buffer for 2 minutes at RT. At the end of cycle 3, slides were immersed in 1 x TTBS buffer overnight at 4°C. Slides were then washed in 1x TTBS buffer 2 times for 2 minutes on the following day before cycle 4 was initiated. At the end of cycle 5, nuclei staining was performed by incubating the slides with DAPI reagent for 5 minutes at RT in a dark chamber. Finally, slides were covered with Vectashield mounting medium and image acquisition was performed.

Target	Color/Filter	Opal	Dilution	Antibody retrieval buffer
CD4	Green/FITC	520	1:200	AR9
CD8	Yellow/Cy3	570	1:300	AR9
CD45RO	Magenta/Cy5	650	1:300	AR6
FoxP3	Orange/Cy5	620	1:450	AR6
CD20	Cyan/Texas Red	540	1:200	AR6

Table 1: Overview of used antibodies in the multiplex staining of five markers

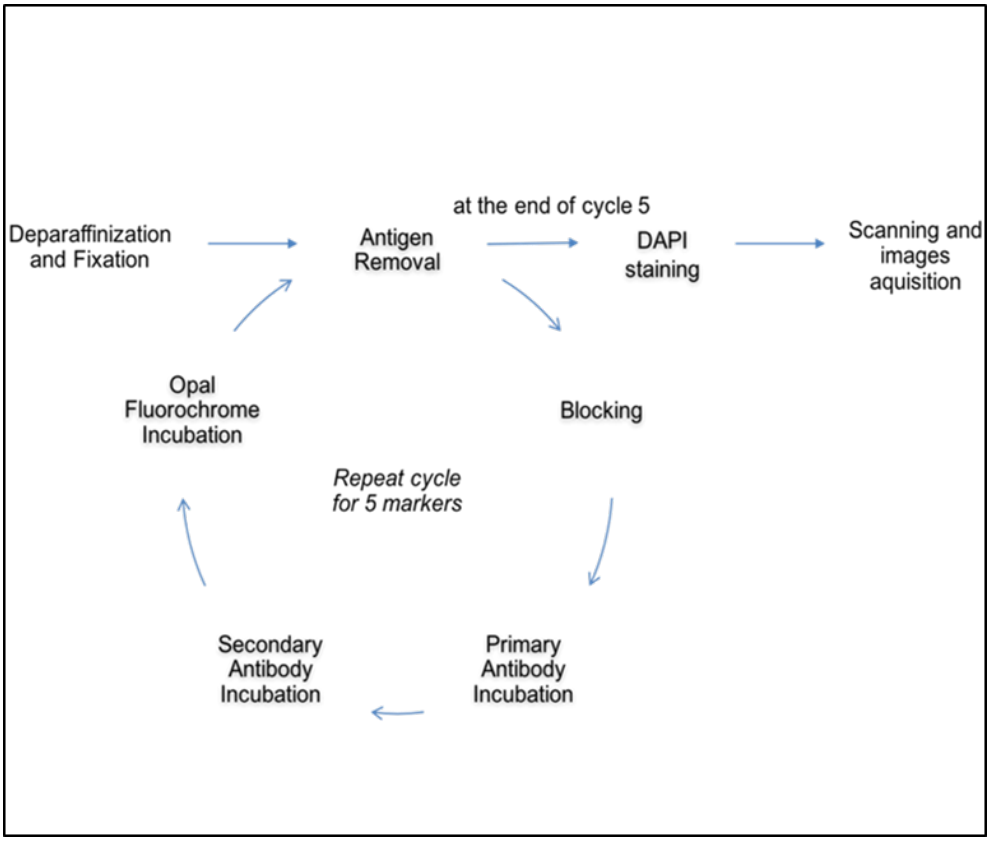

Figure 6. Schematic overview of the immunophenotyping protocol using the Opal 7 Tumor Infiltrating Lymphocytes kit (Akoya Bioscience, Marlborough, MA).

2.2.4 Immunohistochemistry (IHC)

Paraffin sections were dried overnight at 55°C, then deparaffinized and rehydrated according to standard procedure (2 times of 5 minutes each in xylene substitute Neo-Clear, 2 times of 5 minutes each in 100% ethanol, 1 time of 5 minutes each in 95%, 70% ethanol and distilled water). For heat-induced antigen retrieval, slides were brought to boiling temperature in 1x EDTA unmasking solution (for PD-L1 and Tim3 staining) or in 1x Citrate buffer (for PD-1 staining) using a microwave and maintained at a sub-boiling temperature for 15 minutes. After cooling on the bench-top for 30 minutes, slides were washed in distilled water and 1x TTBS buffer each by immersion for 5 minutes at RT. Slides were then incubated with 3% H_2O_2 for 20 minutes at RT followed by incubation in blocking solution (TBST/ 5% normal horse serum) for 1 hour at RT. Primary antibodies were diluted in blocking solution (anti-PD-L1, dilution 1:200; anti-Tim3, dilution 1:250, anti-PD-1, dilution 1:50) and then added to the sections and incubated in a humidified chamber overnight at 4°C. On the following day, slides were then washed three times in 1x TTBS buffer and further processed using the Boost IHC Detection Reagent for 30 minutes at RT. Antigen detection was obtained by a chromogenic reaction with DAB (3-3'- Diaminobenzidine)-staining for 30 minutes at RT. The sections were counterstained with Mayer's hemalum solution for 2 minutes and finally covered with Neo-Mount medium. Representative regions in the stained slides were selected under 10x magnification, and positive cells were counted under 40 x magnifications in five fields of view. The slides were analyzed by two independent reviewers.

2.2.5 Digital Imaging

The stained tissue sections were processed for the whole slide scanning of in a pathology imaging system- Vectra Polaris. Whole slide images were obtained and reviewed by a Phenochart™ software. For downstream analysis, fluroscent images of regions of interest (ROI) were subsequently annotated at 20x magnification in the inform® tissue analysis software. One region of interest was selected for each tissue section by a board-certified pathologist. Filters as FITC, Cy3, Texas Red, and Cy5 were utilized to detect specific opal dyes. One unstained sample was used in each round in order to subtract autofluorescence

and reduce background noise in the inForm software. The number of cytotoxic (CD8+)-, T helper (CD4+)-, regulatory (FOXP3+)- and memory (CD45+)-T cells and B (CD20+)- cells in ROIs were manually quantified by two board-certified pathologists (figure 7 and 8). The counts of five subtypes of immune infiltrates in the examined area were subsequently normalized by the size of ROI (698 µm x 931 µm, a default value in the software).

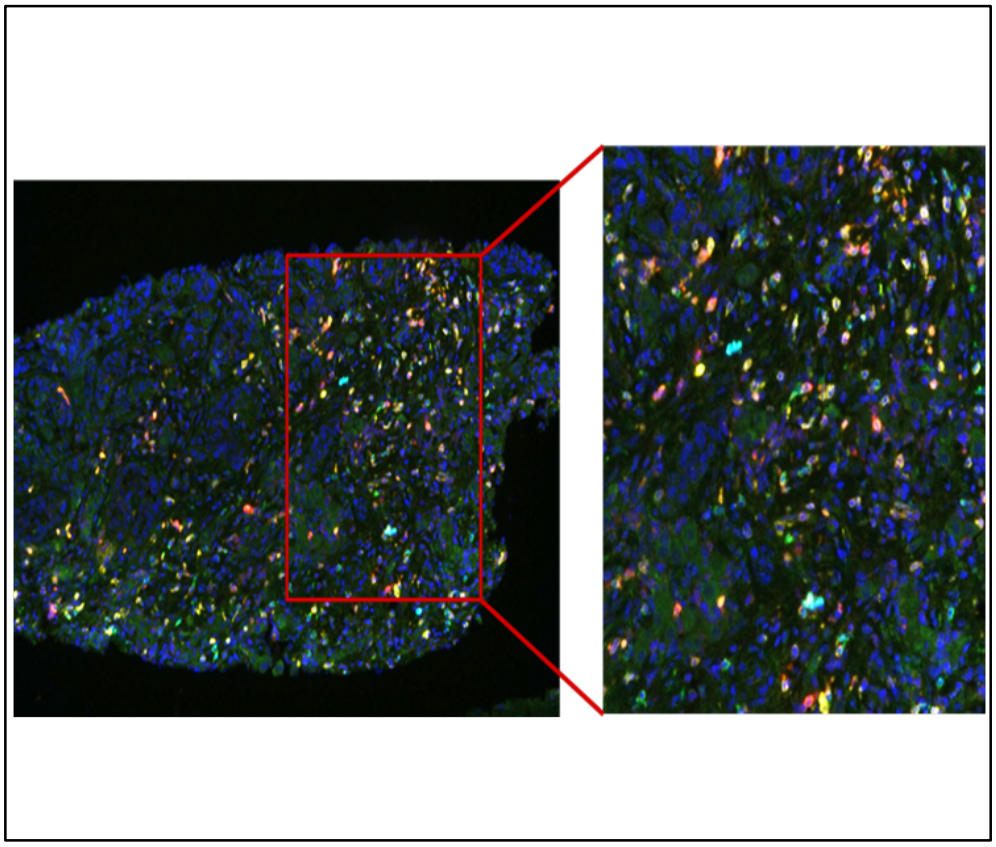

Figure 7. Multispectral representative pictures of ROI (20x magnification). The sample was taken from a pancreatic cancer liver metastasis tissue. Green, yellow, magenta, orange and cyan represent the distribution of cytotoxic (CD8+)-, T helper (CD4+)-, regulatory (FOXP3+)- and memory (CD45+)-T cells and B (CD20+)- cells respectively with the blue background as nuclear staining.

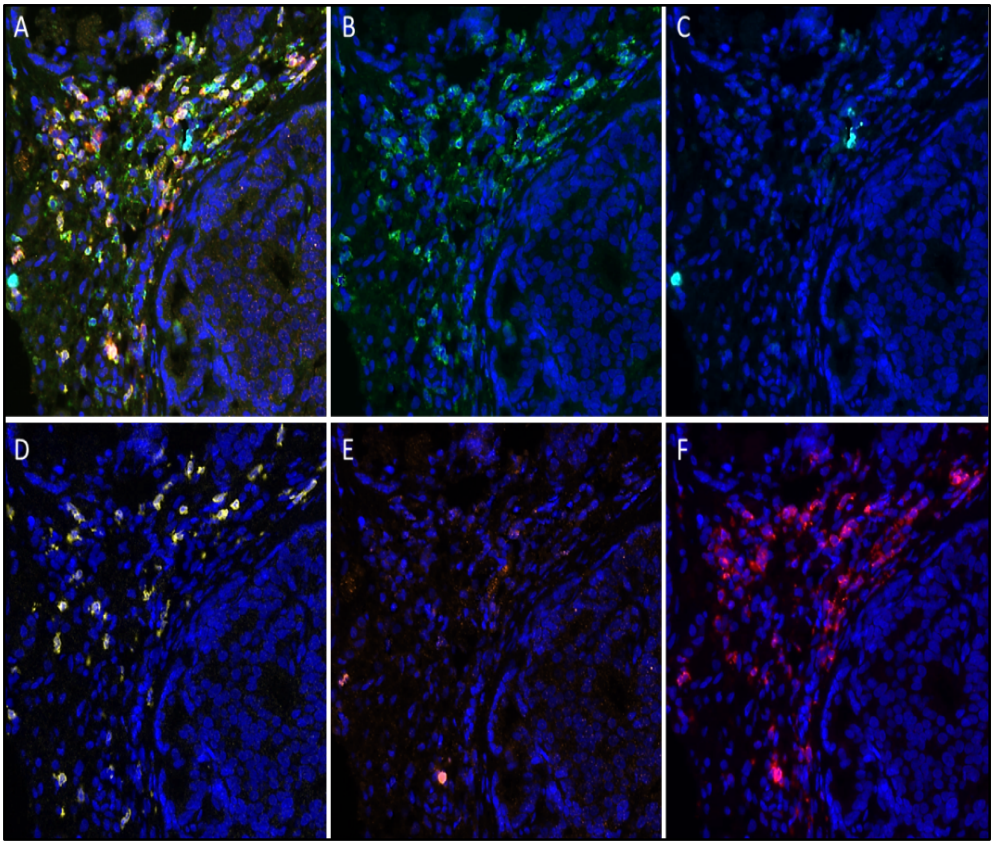

Figure 8. Multiplexed IHC stained liver tissue sample (20x magnification). Staining patterns of individual markers are illustrated in a high-resolution ROI with each cell type represented by a specific color. The composite image encompassing all six colors simultaneously was acquired (A). In five separate channels, distinct markers of CD4 (B, green), CD20 (C, cyan), CD8 (D, yellow), FoxP3 (E, orange) and CD45RO (F, magenta) plus DAPI (dark blue) were characterized, identified and quantified. Four markers (CD4, CD20, CD8 and CD45RO) are located on the cell membrane while FoxP3 as a transcription factor sits in the nucleus.

2.2.5.1 Automatic Counting

In the Vectra Polaris scanning system, a trainable machine-learning algorithm can be set up to carry out automatic cell counting. However, a very high quality of sections and staining is required to enable an automated tissue analysis. In our case, a high variance was present among the samples in terms of thickness and staining density, therefore an algorithm for cell identification and analysis could not be applied. Quantitative counting was therefore performed manually (figure 9).

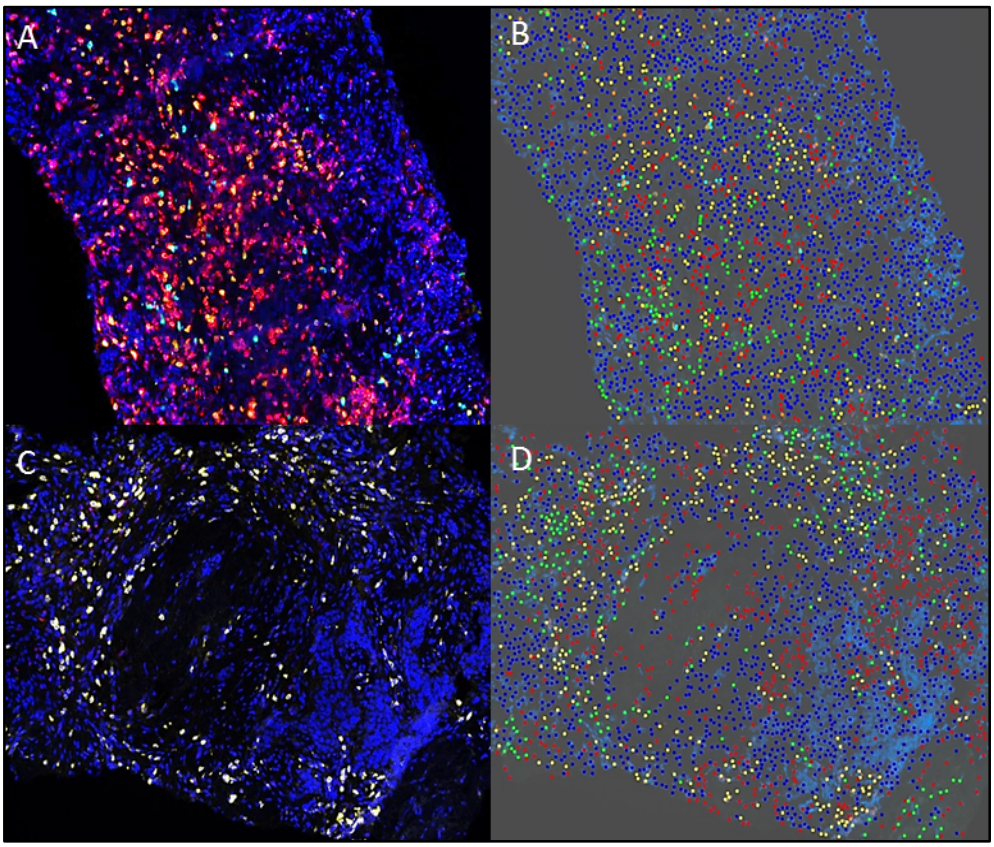

Figure 9. Automatic counting by Vectra Polaris imaging system. All pictures were taken under a microscope with a 20x magnification. (A) digital image of a specific ROI (HCC); (B) image of the same ROI (shown in A) featured by automatic counting; (C) digital image of a specific ROI (pancreatic cancer liver metastasis); (D) image of the same ROI (shown in C) featured by automatic counting. The different colors separate the stained cell phenotypes. Results from automatic machine counting of cell markers indicated a remarkable inconsistency with images obtained under fluorescent microscopy.

2.2.5.2 Manual counting

Multispectral images of ROI were exported from the Inform software and positive cells were qualified and quantified by three independent reviewers using the open source ImageJ analysis program (138). Images were magnified (40x) and adjusted to an optimal degree for better visualization. Stained positive cells in ROIs were then identified and counted manually.

2.2.6 Statistical Analysis

All statistical analyses were performed with IBM SPSS Statistics 21.0.0. The log-rank test was used to compare different patient groups and the Kaplan-Meier method was performed to evaluate overall survival (OS). Overall survival (OS) was calculated for all 27 patients from the date of first radiotherapy until the date of death or of the last traceable follow-up before October 2020. In terms of the relative number of TILs (low TILs subgroup: under the median,

high TILs subgroup: above the median), patients were categorized into two groups for five cell types. The comparison between therapy response and TILs density was analyzed using the Wilcoxon matched-pairs signed-rank test. The non-parametric Mann-Whitney U test was performed to compare two responder groups in terms of the number of TILs both before and after therapy. All tests were carried out two-sided. A p-value <0.05 was considered statistically significant.

2.3. Study design

2.3.1 Patient selection

Two cohorts of 27 primary and secondary liver cancer patients (median age (years): 67, range 33-85) from the THIAMAT trial (German Clinical Trials Register-ID: DRKS00010560) and AROMA trial (German Clinical Trials Register-ID: DRKS00009744) were retrospectively recruited in our study. All patients were reviewed during the period from February 2017 to January 2019 in the Department of Radiology, LMU Klinikum (Munich, Germany). Included patients from these two trials suffered from advanced, unresectable hepatocellular carcinoma (n=4) or hepatic metastasis (n=23). The study was approved by the institutional ethical board and carried out in the framework of the Declaration of Helsinki. Informed consent was provided by all participants. The trial design of the AROMA and THIAMAT trials and the consort chart are given in Figure 10.

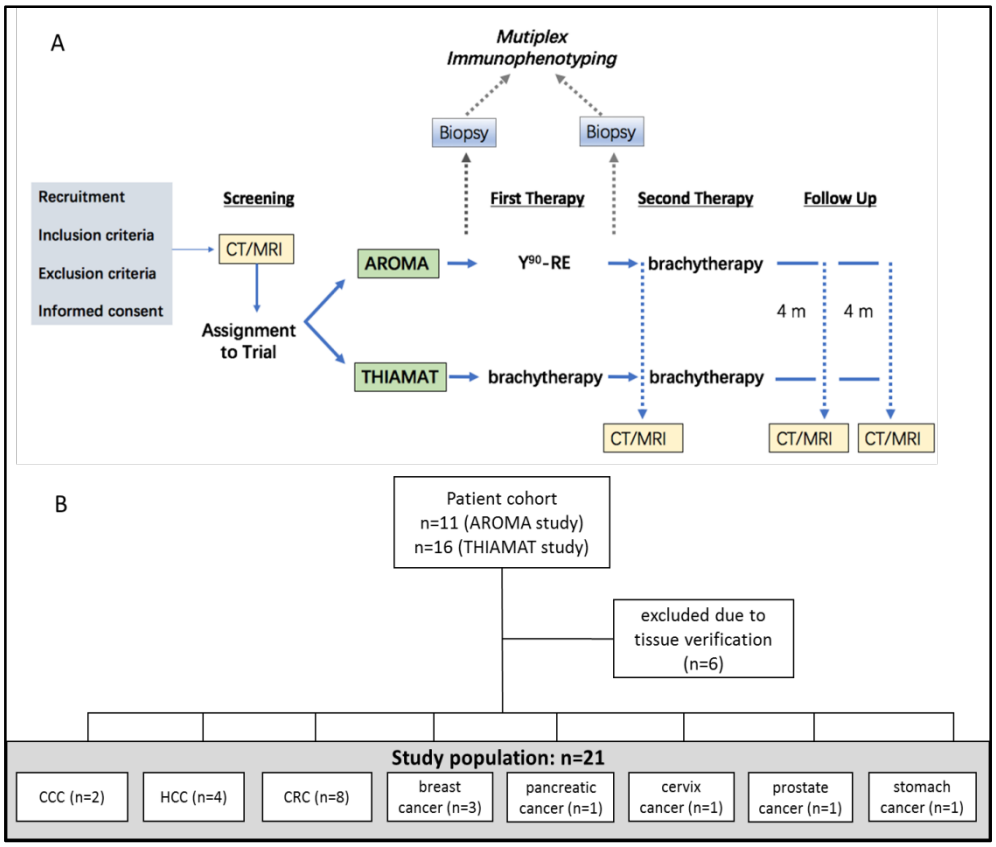

Figure 10. Study design. (A) schematic overview of the clinical workflow. Trial participants who met the inclusion criteria were assigned to the AROMA or THIAMAT arms. Patients included in these two IIT trials went through two sequential therapies. Biopsies of patients were taken before the two therapies respectively. CT or MRI images were collected at three time points: right before the second therapy, 4m follow-up and 8m follow-up, in order to monitor progression of disease. (B) consort chart,

a total of 27 patients was originally recruited in our study, 6 were then excluded due to biopsy control. (Abbreviations: HCC: Hepatocellular carcinoma; CRC: colorectal cancer; CCC, cholangiocellular carcinoma; Y^{90}-RE, Y^{90}-radioembolization)

2.3.2 Patient inclusion and exclusion criteria

Patients' inclusion criteria were:

1) Primary liver cancer or hepatic metastatic cancer (predominantly metastatic colorectal carcinoma)

2) Male or female, > 18 years

3) Indication for radioembolization and High Dose Rate (HDR) -brachytherapy in two sessions

4) Approval of all study procedures

5) Signed informed consent

6) Chemotherapy break for at least two weeks before inclusion

7) Cortisone paused for at least two weeks before inclusion

Patients' exclusion criteria were:

1) Life expectancy< 3 months

2) Extrahepatic tumor manifestation before local ablation treatment

3) Hepatic tumor load >70%

4) Chronic infections (except HBV/HCV infections in HCC patients)

5) Pronounced ascites

6) Contraindication for angiography, MRI contrast media, X-ray contrast media, MRI and CT

7) Liver cirrhosis (in HCC allowed)

8) Status post papilla resection or DHC stent or biliary manipulation

9) Severe cardiovascular disease (NYHA III/IV)

10) Thrombotic or embolic events in the past 6 months (stroke/TIA)

11) Severe hemorrhages within last 3 months

12) Secondary malignomas within last 5 years

13) Immune suppressive therapy or disease (e.g. status post organ transplantation, HIV, corticosteroids)

14) Autoimmune disease or inflammatory bowel disease

15) Cortisone therapy duration

2.3.3 Therapy scheme and biopsy collection

To prevent radiation-induced disease, a six-to-eight week interval was enforced for patients received sequential micro-interventional therapy (MIT). Patients recruited into the THIAMAT trial (n=16) received solely brachytherapy. Patients included into the AROMA trial (n=11) were treated sequentially with brachytherapy and ^{90}Y-radioembolization. Tumor specimens from the treated lobe (L1) and distal, untreated lobe (L2) were taken right before the first and the second therapy (figure 11). Biopsy samples were then stored in 10% Formalin and transferred to the Department of Pathology (LMU Klinikum, Munich, Germany).

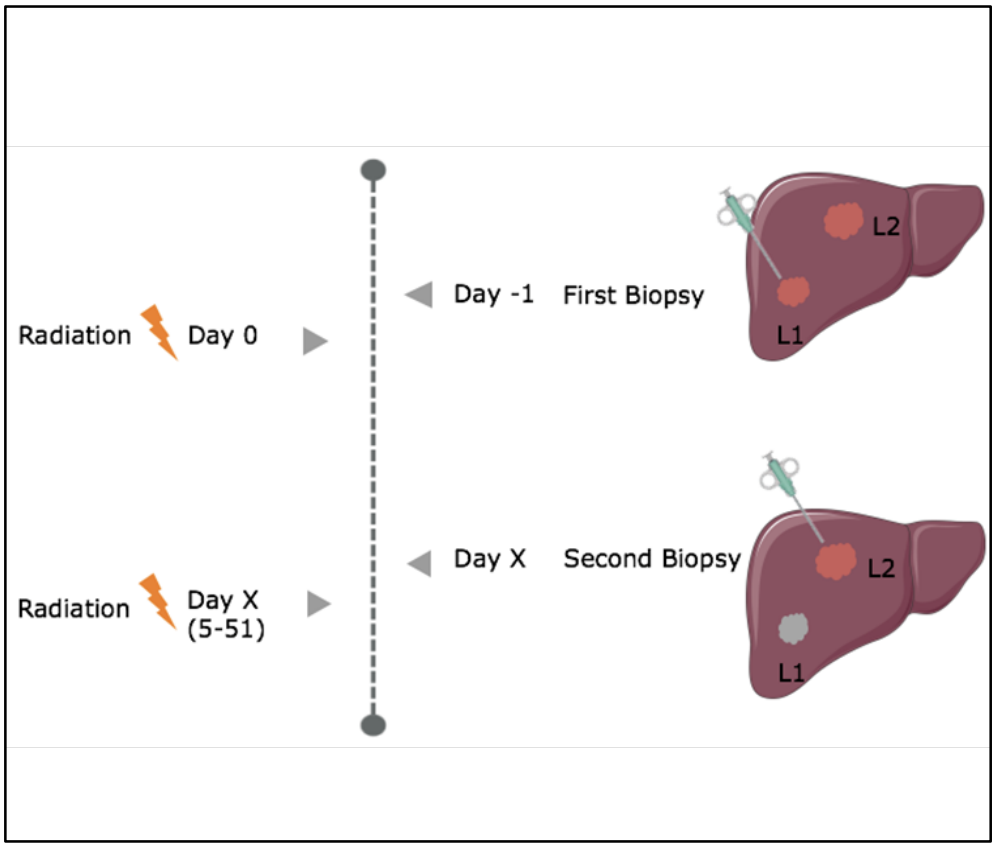

Figure 11. Schematic illustration of liver biopsy. The first and second biopsy were respectively collected at L1 (lesion 1) and L2 (lesion 2) shortly before each therapy.

2.3.4 Classification of response to treatment

The Response Evaluation Criteria in Solid Tumors 1.1 guidelines (RECIST 1.1 criteria)were applied for assessment of patients' radiological response to treatment (139). Patients were sub-grouped and defined as follows:

- Non-responders (NR) (n=14, 58%): patients with progressive disease at 3 months (PD, more than 20% increase in size)
- Transient responders (TR) (n=5, 21%): patients with complete response (CR, no lesion), partial response (PR, more than 30% decrease at 3 months) or stable disease (SD, either less than 30% decrease or lower than 20% increase in size) at 3 months but progressed to PD at 6 months.
- Sustained responders (SR) (n=5, 21%): TR patients without PD at 6 months.

While SR and TR were defined as good responders, NR was considered bad responders.

For three patients, time point imaging was incomplete.

3. Results

3.1 Histological pre-evaluation of lesions

In this study n=27 patients (mean age (years ±SD) 62 ± 13, range 37-83) were recruited from the prospective studies AROMA (n=11) and THIAMAT (n=16). Mean overall survival was 13 months (range 2-37) and mean progression free survival (PFS) was 5 months (range 1-16). Histological analysis of all samples was performed by H&E staining. In 6 cases, biopsies were excluded from the study after H&E evaluation due to extensive tumor necrosis (figure 12A), fragmentation of tissue (figure 12B) or small sample size (smaller than 4x1mm size or fewer than 100 malignant cells in the entire section) (figure 12C). The remaining 21 cases were instead included in our study for further immunophenotyping and immunohistochemical analysis (figure 12D).

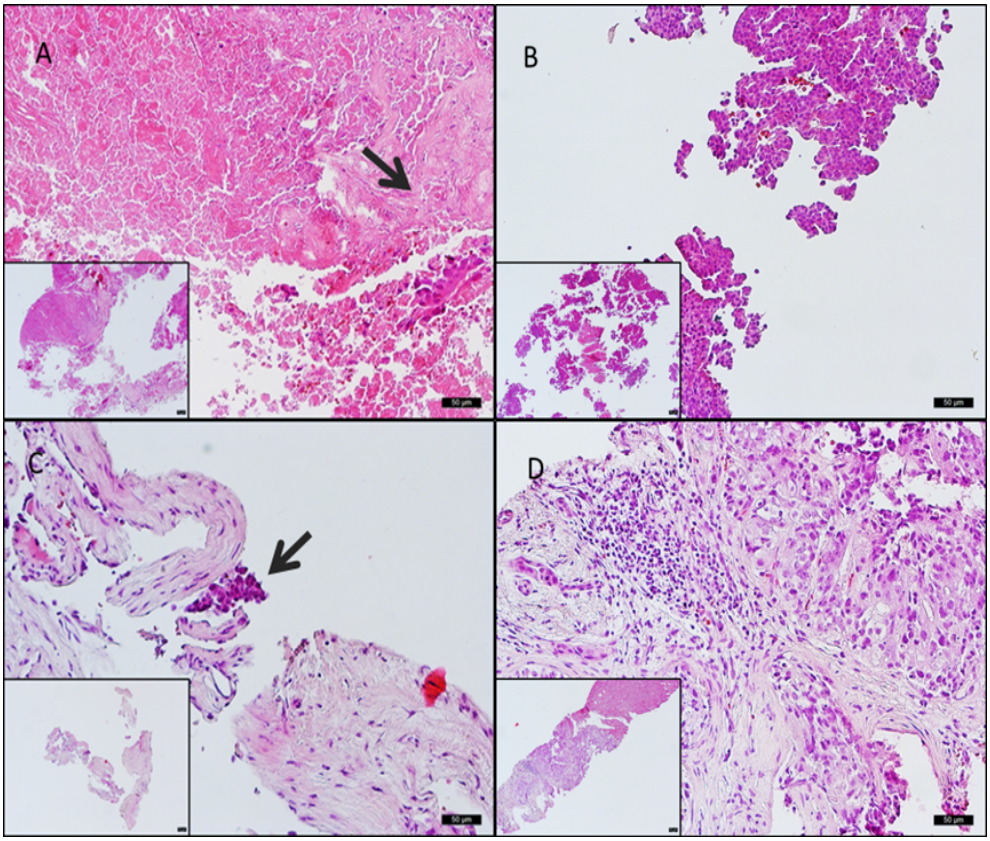

Figure 12: H&E evaluation of the bioptic material collected from patients. 54 samples were analyzed corresponding to 27 patients; few samples were excluded from further analysis due to: (A) extensive necrosis and small tumor cluster (arrow); (B) the presence of fragmented tumor clusters without stromal areas; or (C) small tumor cluster (arrow) with stromal fragments. Biopsy samples that showed sufficient tumor tissue and presence of

immune cells in between tumoral areas were instead included (D) Larger images were investigated at 20x magnification, while small images were investigated at 5x magnification. All scale bars are equal to 50µm.

3.2 Clinical characteristics of patients

n=15 liver metastasis patients were diagnosed with colorectal (n=8, 52%), breast (n=3, 20%), cervical (n=1, 7%), pancreatic (n=1, 7%), stomach (n=1, 7%), and prostate (n=1, 7%) cancer as primary tumor. Patients with cholangiocellular carcinoma (n=2) were included into the non-HCC subgroup as well. In addition, 4 primary HCC patients were included in the cohort as a separate sub-group. Patient details and primary tumor characteristics are presented in table 2.

Results

Characteristics	No. of patients (%)							
Organ with primary cancer	Breast	Pancreatic	Stomach	Colon	Prostate	Cervix	CCC	HCC
Total number	3	1	1	8	1	1	2	4
Age, y								
Mean±SD	68±16	73	63	58±11	73	79	56±26	59±12
Range	52-80	73	63	38-71	73	79	33-84	50-79
T stage								
pT1-T2	2 (67)	0 (0)	0(0)	1 (13)	0(0)	0(0)	0(0)	-
pT3	0(0)	1(100)	1(100)	4 (50)	1(100)	0(0)	1(50)	-
Unknown	1 (33)	0(0)	0(0)	3 (37)	0(0)	1(100)	1(50)	-
N stage								
N0	1 (33)	0(0)	0(0)	1 (13)	0(0)	0(0)	0(0)	-
N1	1 (33)	1(100)	1(100)	4 (50)	1(100)	0(0)	0(0)	-
N2	0(0)	0(0)	0(0)	1 (13)	0(0)	0(0)	0(0)	-
Unknown	1 (33)	0(0)	0(0)	2 (24)	0(0)	1(100)	2(100)	-
UICC(Stadium)								BCLB stage
0-III	0(0)	0(0)	0(0)	0(0)	0(0)	0(0)	1(50)	A 0(0)
IV	0(0)	0(0)	0(0)	5 (63)	0(0)	0(0)	1(50)	B-C 4(100)
Unknown	3 (100)	1(100)	1(100)	3 (37)	1(100)	1(100)	0(0)	
Histological grading								CP
G1-2	1 (33)	0(0)	1(100)	2 (24)	0(0)	0(0)	1(50)	A 1(25)
G3	1 (33)	1(100)	0(0)	1 (13)	1(100)	1(100)	0(0)	B 1(25)
Unknown	1 (33)	0(0)	0(0)	5 (63)	0(0)	0(0)	1(50)	C 2(50)
VELIPI								PVI
No	0(0)	0(0)	0(0)	2 (24)	0(0)	0(0)	0(0)	1(25)
Yes	0(0)	1(100)	1(100)	1 (13)	1(100)	0(0)	1(50)	3(75)
Unknown	3 (100)	0(0)	0(0)	5 (63)	0(0)	1(100)	1(50)	0(0)
Tumor marker								
AFP High	na	na	na	na	na	na	2(100)	3(75)
low							0	1(25)
PSA high	na	na	na	na	1(100)	na	na	na
CA15-3 high	2 (67)	na	na	1 (13)	1(100)	na	na	na
low	1 (33)			7 (87)	0 (0)			
CA19-9 high	na	1(100)	0(0)	6 (76)	na	0(0)	0(0)	na
low		0(0)	1(100)	2 (24)		1(100)	2(100)	
Pre-treatment								
No	0(0)	0(0)	0(0)	0(0)	0(0)	0(0)	1(50)	4(100)
Yes	3 (100)	1(100)	1(100)	8 (100)	1(100)	1(100)	1(50)	0(0)
Mutation	na	na	na	K-RAS 3 (37)	na	na	na	na
Hormone receptor status								
Negative	1 (33)	na	na	na	na	na	na	na
Positive	2 (67)							
HER2 status								
Negative	1 (33)	na	1(0)	na	na	na	na	na
Positive	2 (67)		0(100)					
Other	-	-	-	lung metastasis 3(37)	Gleason p=7	-	-	Cirrhosis 3 (75) HCV 1(25) NASH 1(25)

BCLC, Barcelona Clinic Liver Cancer; CP, Child-Pugh; PVI, portal vein infiltration; Nash, non-alcoholic steatohepatitis; VELIPI: vascular emboli (VE), lymphatic invasion (LI), perineural invasion (PI), alone or in combination; na, not available

Table 2. Clinico-pathological characteristics of the patients

Results

Patients with multiple lobular lesions (n=6, 29% with <5 lesions, n=15, 71% with >= 5 lesions, mean size 3.6cm, range 1.5-7.6) received two sequential cycles of therapy (SIRT followed by brachytherapy for the AROMA sub-cohort and two successive brachytherapies for the THIAMAT sub-cohort) within a time frame of 5-51 days (mean: 16 days). Table 3 displays a summary of the patient clinical characteristics.

No	Pat ID	Sex	Age	Primary Tumor	OS (M)	PFS (M)	4m RECIST	8m RECIST	RS	biggest lesion(cm)	Number of lesion
AROMA											
1	RAD202	m	53	HCC	7	4	PD	PD	NR	3.1	Multiple
2	RAD206	f	71	Pancreatic	4	1	PD	PD	NR	2.8	Multiple
3	RAD208	f	31	CCC	27	3	PD	PD	NR	3	Multiple
4	RAD207	f	75	Breast	10	6	SD	PD	TR	4	Multiple
5	RAD210	f	50	Breast	7	2	PD	PD	NR	2.3	Multiple
6	RAD209	f	63	Sigma	16	13	SD	SD	SR	3.7	Multiple
7	RAD212	m	65	Sigma	2	2	PD	PD	NR	7.6	Multiple
8	RAD215	f	61	Rectal	5	1	PD	PD	NR	6.1	Multiple
THIAMAT											
9	RAD502	m	68	Sigma	13	10	SD	SD	SR	3.1	3
10	RAD504	f	62	Cecum	37	4	PD	PD	NR	2.8	Multiple
11	RAD531	m	37	Sigma	23	4	PD	PD	NR	2.8	Multiple
12	RAD557	f	62	Rectal	4	4	NA	NA	NA	3.3	5
13	RAD558	m	50	Rectal	12	2	PD	PD	NR	3.8	Multiple
14	RAD509	m	77	HCC	17	8	PR	PR	SR	3.7	2
15	RAD511	m	56	HCC	17	5	SD	PD	TR	3.5	Multiple
16	RAD561	m	50	HCC	11	11	PR	PR	SR	3.8	3
17	RAD544	f	63	Stomach	12	2	PD	PD	NR	3.9	4
18	RAD518	f	78	Cervix	7	2	PD	PD	NR	2	Multiple
19	RAD519	f	79	Breast	25	3	PD	PD	NR	4.7	4
20	RAD520	m	71	Prostate	26	16	PR	CR	SR	1.5	4
21	RAD524	m	83	CCC	13	4	SD	PD	TR	4.5	5

m, male; f, female; HCC, hepatocellular carcinoma; CCC, cholangiocellular carcinoma; NET, neuroendocrine tumor; OS, overall survival; PFS, progression-free survival; PR, partial response; PD, progressive disease; SD, stable disease; NR, non-responder; TR, transient-responder; SR, sustained responder; RS, response status; NA, not available.

Table 3. Patient journey of enrolled patients.

3.3 Radiotherapy induces changes in the immune landscape

In order to evaluate the local immune response to radiotherapy, immune infiltration was analyzed on FFPE (formalin fixed and paraffin embedded)-tissue samples from adjacent tumor lesions (lesion 1, L1 and lesion2, L2) by quantification of the expression of five different markers for TILs (CD20, CD4, CD8, CD45RO and FoxP3) in the region of interest. L1 and L2 were considered to be histologically comparable before the first therapy was induced. Median values of TILs densities in L1 and L2 were as follows (/mm^2): CD20: 27.73 (95%CI= 81.2 $\pm$ 53.1) and 15.41(95%CI= 81.2 $\pm$ 53.1); CD4: 40.06 (95%CI= 104.5 $\pm$ 53.7) and 30.82 (95%CI= 97.0 $\pm$ 67.1); CD45RO: 132.51(95%CI= 225.7 $\pm$ 99.6) and 101.69 (95%CI= 163.2 $\pm$ 67.8); CD8:117.69 (95%CI= 136.2 $\pm$ 43.8) and 70.88 (95%CI= 143.8 $\pm$ 69.4); FoxP3: 7.70 (95%CI= 19.1 $\pm$ 11.7) and 6.16 (95%CI= 16.5 $\pm$ 11.4), whereas the mean values of TILs density at both time points (/mm^2) were as follows: CD20: 81.16 and 39.31; CD4: 104.53 and 97.05; CD45RO: 225.74 and 163.18; CD8:136.16 and 143.82; FoxP3: 19.08 and 16.46 (table 4).

Pat No.	Time frame (d)		Cell count(/mm²)									
			CD20		*CD4*		*CD45RO*		*CD8*		*FOXP3*	
AROMA		Tumor	L1	L2	L1	L2	L1	L2	L1	L2	L1	L2
2	55	Pancreatic	27,73	9,24	292,76	86,29	494,61	360,55	83,20	69,34	73,96	6,16
3	26	CCC	10,79	0,00	40,06	6,16	121,73	78,58	234,21	585,52	10,79	9,24
4	28	Breast	4,62	4,62	144,84	6,16	80,12	69,34	81,66	47,77	6,16	1,54
5	15	Breast	0,00	1,54	0,00	41,60	57,01	46,22	46,22	44,68	24,65	10,79
6	27	Sigma	4,62	0,00	7,70	4,62	23,11	101,69	411,40	70,88	3,08	3,08
7	33	Sigma	0,00	20,03	0,00	6,16	0,00	6,16	137,13	471,49	3,08	1,54
8	29	Rectal	0,00	0,00	0,00	0,00	7,70	0,00	0,00	7,70	0,00	0,00
1	30	HCC	13,87	72,42	132,51	215,72	825,89	117,70	86,29	40,06	23,11	6,16
THIAMAT		Tumor	L1	L2	L1	L2	L1	L2	L1	L2	L1	L2
9	14	Sigma	90,91	73,96	6,16	9,24	86,29	488,44	52,39	137,13	6,16	4,62
10	14	Cecum	67,80	3,08	18,49	0,00	84,75	30,82	100,15	35,44	0,00	0,00
11	5	Sigma	64,71	258,86	12,33	21,57	7,70	192,60	214,18	237,29	0,00	0,00
12	19	Rectal	48,46	10,38	171,54	390,38	221,54	333,08	120,77	160,38	83,85	25,38
13	13	Rectal	21,92	79,49	200,38	506,67	235,38	428,72	117,69	226,15	17,69	90,77
17	24	Stomach	236,92	29,62	367,69	358,46	294,62	333,85	122,69	96,92	10,77	26,92
18	16	Cervix	24,65	6,16	123,27	30,82	132,51	30,82	112,48	32,36	30,82	38,52
19	14	Breast	12,33	15,41	97,07	63,17	217,26	226,50	292,76	283,51	67,80	80,12
20	14	Prostate	29,28	10,79	40,06	21,57	118,64	92,45	73,96	60,09	0,00	6,16
21	11	CCC	363,64	92,45	18,49	63,93	382,13	184,90	32,36	7,70	0,00	3,08
14	23	HCC	197,23	15,41	38,52	3,08	599,38	4,62	224,96	53,93	7,70	10,79
15	15	HCC	388,29	67,80	115,56	35,44	425,27	69,34	137,13	229,58	0,00	4,62
16	14	HCC	96,54	54,23	367,69	166,92	325,00	230,38	177,69	122,31	31,15	16,15
MEDIAN	16		27,73	15,41	40,06	30,82	132,51	101,69	117,69	70,88	7,70	6,16
MEAN	21		81,16	39,31	104,53	97,05	225,74	163,18	136,16	143,82	19,08	16,46
SD	11.72		116,54	59,08	117,97	147,75	218,88	148,98	96,12	152,45	25,70	25,08
p			0.095		0.481		0.288		0.759		0.863	

Table 4. Quantification of TILs in lesion 1 and lesion 2. Five TILs subtypes were counted, normalized by the size of region of interest in both L1 and L2. Median value, mean value and standard deviation (SD) were calculated for each cell type. Increase and decrease in TILs density were indicated in red and in blue respectively.

Intra-patient analysis showed that in more than 50% of the patients from the non-HCC cohort the relative number of the analyzed TILs decrease or did not show any difference in in L2 compared to L1. A similar trend was also observed in HCC patients (figure 13). Despite a decline seen for more than half of the patients in both cohorts, an increased immune infiltration was still demonstrated in 29% (CD20), 41% (CD4), 47% (CD45RO), 41% (CD8), and 35% (FoxP3) of liver metastasis cohort as well as 25% (CD20), 25% (CD4), 0% (CD45RO), 25% (CD8) and 50% (FoxP3) in the HCC group.

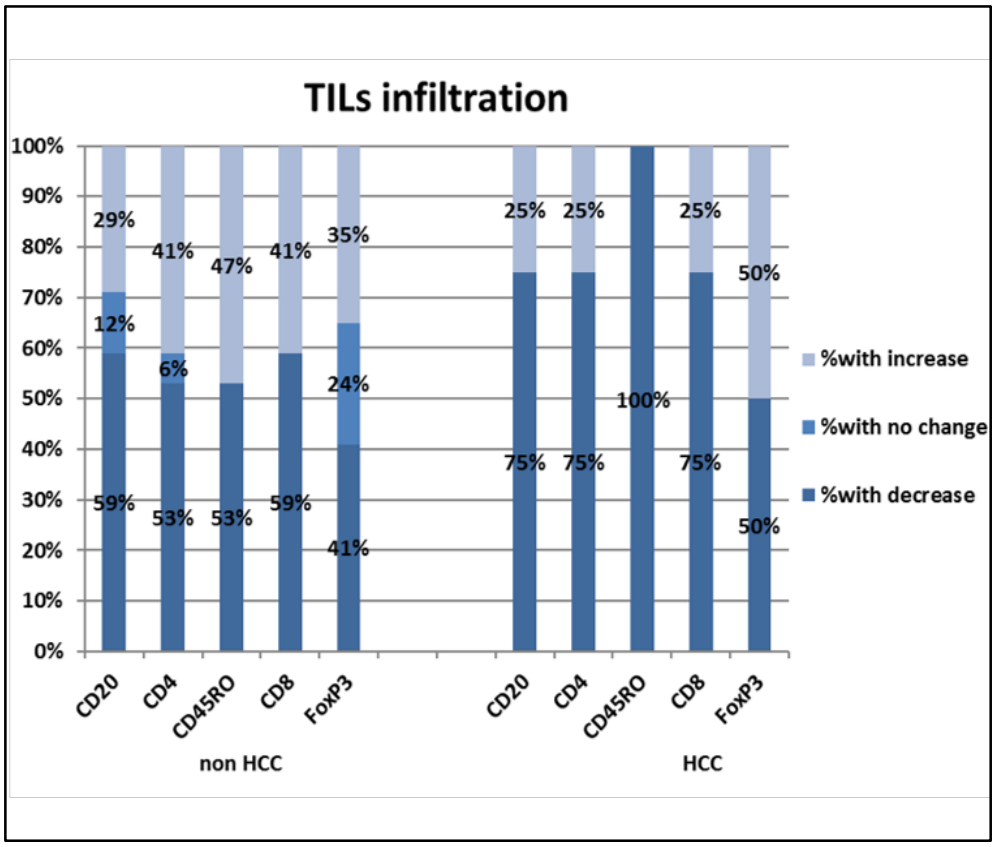

Figure 13. Amount of TILs in L2 compared to L1. The percentage change of CD20, CD4, CD45RO, CD8 and FoxP3, and TILs subgroups in both the non-HCC cohort and the HCC cohort.

Irrespective of the primary tumor, the most represented cell type in both lesions was CD45RO (41% in L1 and 45% in L2), followed by CD8 (36% in L1 and 31% in L2), CD4 (12% in L1 and 14% in L2), CD20 (9% in L1 and 7% in L2) and FoxP3 (2% in L1 and 3% in L2) (figure 14).

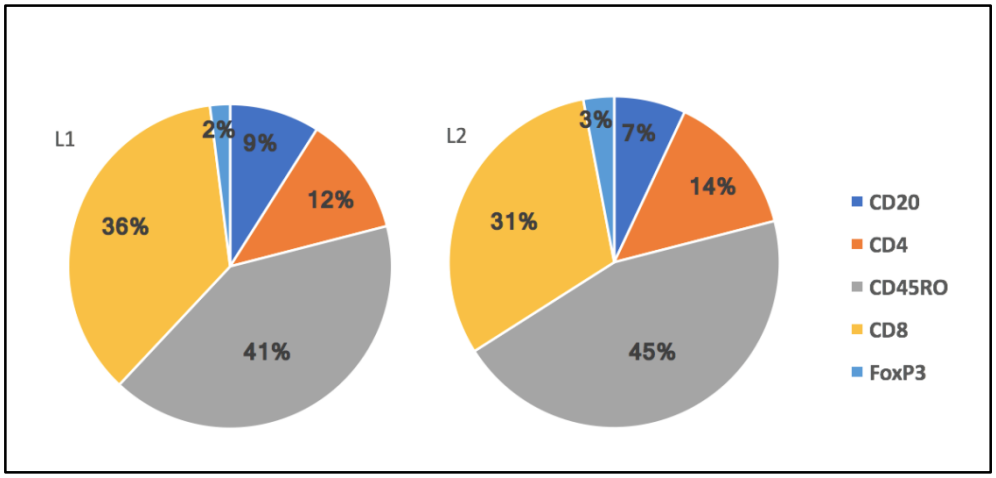

Figure 14. Percentage of TILs distribution in tumor microenvironment. The relative amounts of $CD20^+$, $CD4^+$, $CD45RO^+$, $CD8^+$ and $FoxP3^+$ TILs were calculated at both time points. $CD8^+$ and $CD45RO^+$ took up the largest proportion in the investigated tumor microenvironment, followed by $CD4^+$, $CD20^+$ and $FoxP3^+$.

3.4 Immune cell infiltrates distribution within the tissue

To evaluate the distribution of TILs in the lesions, the localization pattern of TILs in ROI was analyzed for each sample. Prominent variations in the density and distribution pattern were observed both at the center of tumor (CT) and in the invasive margin (IM). In several cases of liver metastasis, the tissue analysis evidenced a clear concentration of immune infiltrates in IM of the intra-tumoral or peri-tumoral areas while they were missing almost completely in CT. In addition, in contrast to biopsies from HCC where extensive and diffuse immune infiltration was observed, a higher grade of TILs infiltration was present only in the peripheral area of liver metastasis (figure 15).

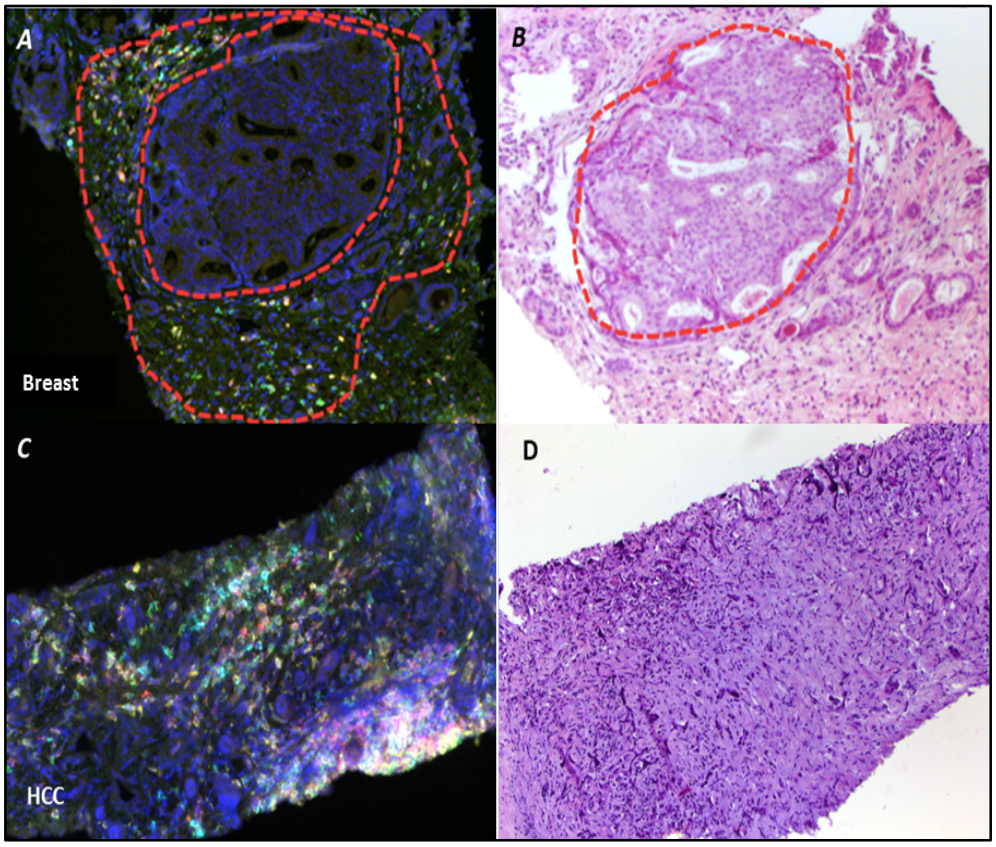

Figure 15. Representative examples of TILs infiltration in primary and secondary liver cancer. In liver metastasis, (A) TILs were distributed only in the invasive margin of intra-tumoral or peri-tumoral regions while TILs were almost absent in the core region of the tumor. (C) On the contrary, a homogenous infiltration of TILs in the whole tissue was detected in HCC. (B and D) H&E staining was performed on the same tissues as control.

3.5 Prognostic value of TILs

To evaluate the prognostic value of TILs detected in the lesions, Kaplan-Meier analysis was performed. We observed that the amount of CD20 in L2 was negatively associated with OS (p=0.048), which suggested that patients holding a higher amount of $CD20^+$ TILs in L2 could have a worse prognosis. No association was detected between overall survival and other single cell markers at both time points. The ratios based on two cell subgroups out of $CD4^+$, $CD8^+$, $CD20^+$, $CD45RO^+$ and $FOXP3^+$ TILs were also calculated in both lesions L1 and L2. In L1, although it was not statistically significant, high CD8/CD45RO and low CD20/CD8 ratios showed a borderline (p=0.093 and p=0.080, respectively) association with a favorable clinical outcome. In L2, a trend was observed that a high CD4/CD45RO ratio correlated to a worse prognosis (p=0.068). No other significant results were found (table 5). HCC patients were not included for analysis in this case, due to the small cohort size.

Marker	L1		L2	
	Median OS (months)	p-values	Median OS (months)	p-values
$CD4^+$				
High	10	0.829	8	0.670
Low	14.5		13	
$CD8^+$				
High	23	0.334	17.5	0.477
Low	11		12	
$CD45RO^+$				
High	12	0.993	12.5	0.235
Low	13		10	
$FoxP3^+$				
High	7	0.660	12	0.746
Low	13		13	
$CD20^+$				
High	13	0.201	13	***0.048***
Low	8.5		10	
$CD4^+$:$CD8^+$				
High	8.5	0.157	12	0.458
Low	16		14.5	
$CD4^+$:$CD45^+$				
High	12	0.682	7	***0.068***
Low	12.5		14.5	
$CD4^+$:$CD20^+$				
High	12	0.180	10	0.380
Low	13		14.5	
$CD20^+$:$CD8^+$				
High	13	***0.080***	18	0.143
Low	11		12	
$CD20^+$:$CD45^+$				
High	18	0.150	10.5	0.642
Low	12		12	
$CD8^+$:$CD45^+$				
High	24	***0.093***	24	0.839
Low	7		12	
$Foxp3^+$:$CD20^+$				
High	8.5	0.792	7	0.937
Low	13		13	

Table 5. Correlation between TILs and clinical outcome.

3.6 Correlation between the density of TILs and therapy response

In our cohort, patients who received radiotherapy were classified into three subgroups: SRs, NRs and TRs. These patients were further defined as good responders (SRs) and bad responders (NRs and TRs) respectively. No significant difference was discovered in any investigated cell subgroup when two groups of responders were compared (all $p>0.05$). Meanwhile, no significant change was detected for each TIL type within each individual

responder group (all p>0.05). The whole cohort (including HCC patients) and the non-HCC group only were used for the analysis.

3.7 Quantification of exhaustion markers PD-1, PD-L1 and Tim3

In order to investigate the possible mechanism behind the changes in the immune landscape after patients received therapy, the expression level of three well-established immune exhaustion markers PD-L1, PD-1 and Tim3 was examined individually. The presence of the three markers was also evaluated with respect to their distribution in both tumor cells and in tumor microenvironment at both lesions. The expression level of Tim3 positive tumor cells was significantly higher in L2 (p=0.012). Additionally, tumor cells positive for PD-L1 declined substantially after the therapy (p=0.016). On the contrary, no significant change was revealed in terms of the expression of PD-1 positive tumor cells between L1 and L2 (figure 16). The positive cells for each of the three markers in TME were quantified analogously. No other statistically significant difference was shown comparing two lesions (p>0.05). The HCC cohort was not included for the analysis due to the small cohort size (only two patients were eligible for staining of exhaustion markers).

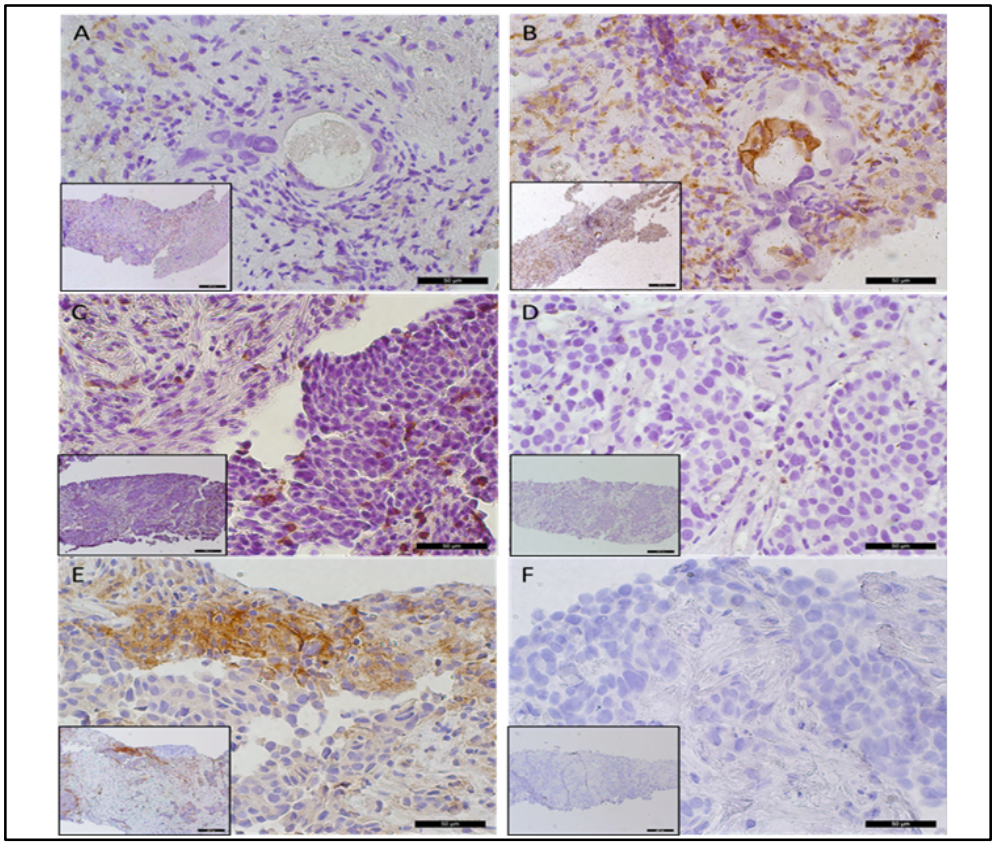

Figure 16. Expression of Tim3, PD-1 and PD-L1 in liver metastasis. The expression of the markers was evaluated based on staining of tumor cells and tumor microenvironment. (A) Low concentration of Tim3 in tumor cells in L1; (B) high concentration of Tim3 in tumor cells in L2; (C) high concentration of PD-1 in TILs and macrophages in L1; (D) low concentration of PD-1 in TILs and macrophages in L2; (E) high concentration of PD-L1 in tumor cells in L1; (F) low concentration of PD-L1 in L2.

To explore the correlation between clinical outcome and each type of exhaustion markers, Kaplan-Meier analyses were performed at both time points. Patients showing higher numbers of PD-1 positive cells in TME in L2 were shown to have a longer overall survival (p=0.045) (Figure 17). However, no significant correlation between overall survival and the expression level of Tim3 and PD-L1 was detected in both lesions (all p>0.05).

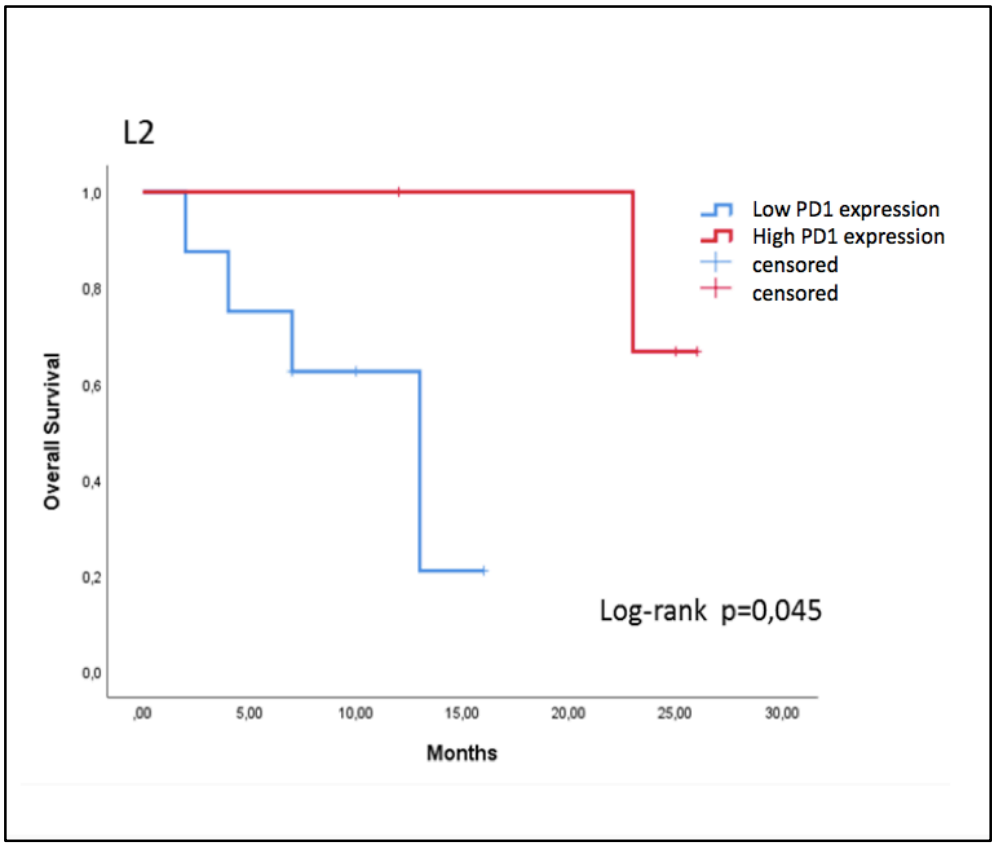

Figure 17. Kaplan-Meier plot of OS according to high and low PD-1 expression in TME. Patients presenting a higher amount of PD-1 positive cells in TME in L2 had a prolonged survival rate (p=0.045).

3.8 Detection of abscopal effect

To detect the occurrence of a possible positive abscopal effect in the cohort chosen for the study, and to evaluate a possible association with the lymphocyte infiltration of the

untreated lesion L2, the CT and the MRI images obtained shortly before the first and the second therapy were reviewed to measure changes in the size of the lesion according to the RECIST criteria. Only 7 patients had images traceable at aforementioned two time points. Among them, 4 patients showed Progressive Disease (PD, an increase in diameter higher than 20%) in L2 after the first therapy. The remaining three patients displayed Stable Disease (SD, neither sufficient shrinkage nor enlargement) in L2. To better illustrate the features of MRI images and the corresponding changes in immunophenotyping, three specific cases are discussed. An overview of patients' history is given in Table 6.

Patient 3 (female, age 75) (Fig 21)	1999 First diagnosis of breast cancer
	08.2014 Detection of liver metastasis
	12.02.2018 Implementation of SIRT
	13.03.2018 Implementation of brachytherapy
	03.05.2018 Stable disease
	03.08.2018 Progressive disease
Patient 13 (female, age 62) (Fig 22)	diagnosis of colorectal cancer (date not available)
	12.2015 Detection of liver metastasis
	31.08.2017 Implementation of first cycle of brachytherapy
	14.09.2017 Implementation of second cycle of brachytherapy
	21.12.2017 Progressive disease
Patient 14 (male, age 77) (Fig 23)	10.2017 diagnosis of HCC
	08.01.2018 Implementation of first cycle of brachytherapy
	31.01.2018 Implementation of second cycle of brachytherapy
	24.04.2018 Partial response
	21.06.2018 Partial response

Table 6. Patient clinical history

Case 1(patient 3, AROMA) (figure 18)

The patient was diagnosed with breast cancer liver metastasis and classified as a TR (4m RECIST SD, 8m RECIST PD). After radiotherapy, a reduction in TILs number was observed in L2 with respect to L1 (CD4 -96%, CD45RO -13%, CD8 -41%, FoxP3 -75%

while no difference was detected for B cells. In MRI images, PD (Progressive Disease, an enlargement of 30% in the size) was noted in L2.

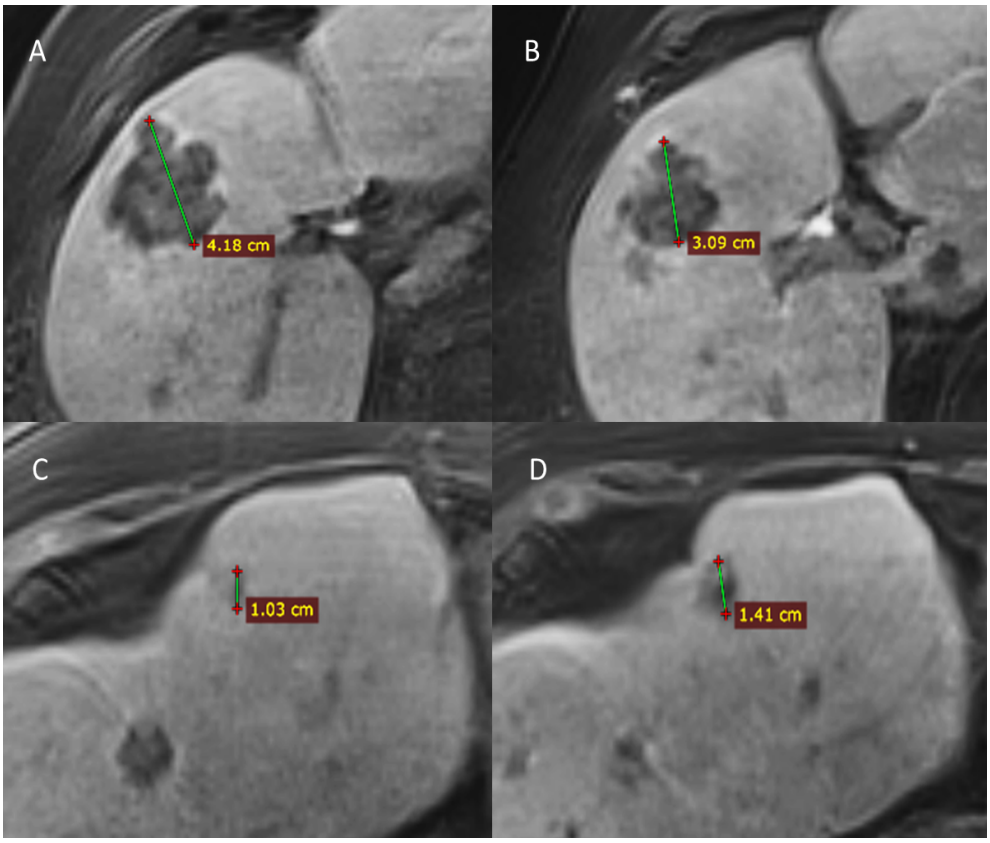

Figure 18. T1w contrast-enhanced hepatobiliary phase MRI images of patient 3 (breast cancer liver metastasis). (A) L1 before the first therapy; (B) L1 before the second therapy; (C) L2 before the first therapy; (D) L2 before the second therapy. The dynamic change in the size of L2 (C→D) was shown whereas a decrease in lesion 1 (A→B) was displayed. The diameter of L2 increased from 1.03 cm (C) to 1.41 cm (D) (an increase of 30%) after the first therapy.

Case 2 (patient 13, THIAMAT) (Figure 19)

The patient was diagnosed with colorectal cancer liver metastasis and classified as a NR (4m RECIST PD). The immunophenotyping results showed a decrease for all cell subgroups (CD20 -95%, CD4 -100%, CD45RO -64%, CD8 -65%), while no change was observed for FoxP3^{+} T cells (0%). A minimal change of only 0.4% (T1 2.40cm, T2 2.41cm) in the size of L2 was seen in MRI images.

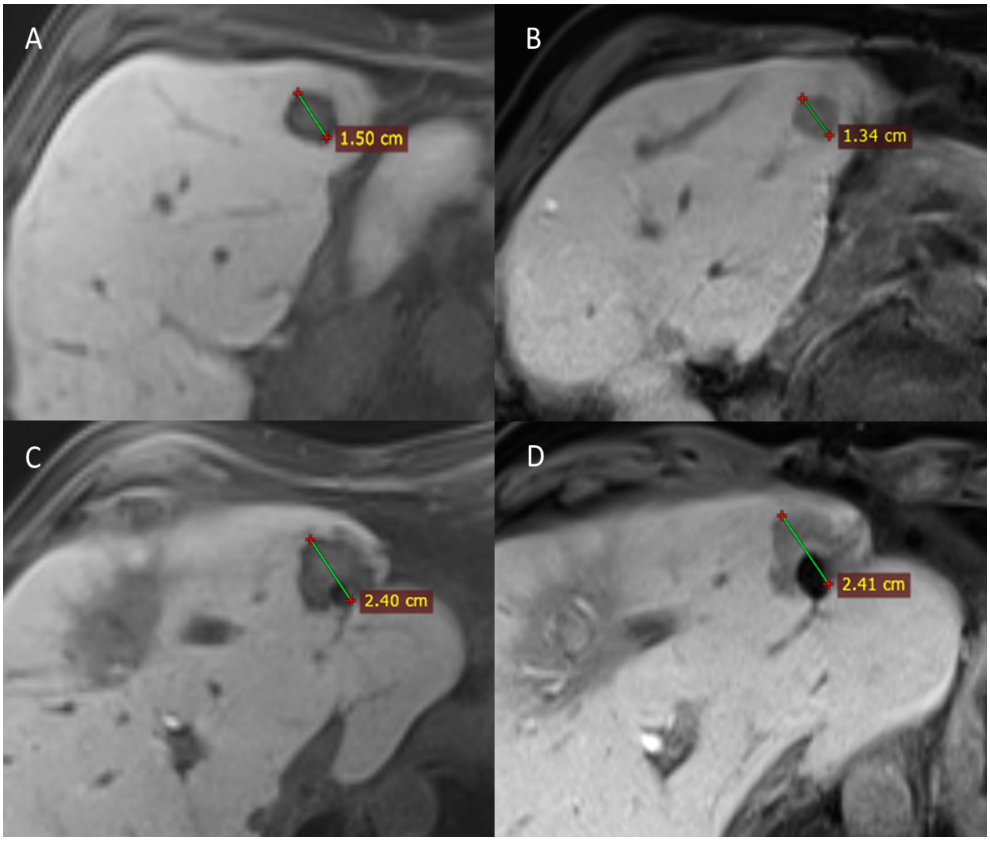

Figure 19. T1w contrast-enhanced hepatobiliary phase MRI images of patient 13 (colorectal cancer liver metastasis). (A) L1 before the first therapy; (B) L1 before the second therapy; (C) L2 before the first therapy; (D) L2 before the second therapy. The diameter of L2 increased from 2.40 cm (C) to 2.41 cm (D) (an increase of 0.4%) after the first therapy.

Case 3 (patient 14, THIAMAT) (Figure 20)

The patient was diagnosed with HCC and classified as a SR (4m RECIST PR, 8m RECIST PR). A clear reduction of CD20 (-60%) and CD45RO (-70%) was observed in L2, while in the same lesion a strong increase of CD4 (+484%), CD8 (+203%) and FoxP3 (+133%) was observed. In MRI images, a slight decrease of 12% (T1 1.63cm, T2 1.43cm) in the size of L2 was detected. However, being less than 30% in the change of the size, this reduction cannot be qualified as Partial Response (PR).

Figure 20. T1w contrast-enhanced MRI images of patient 14 (HCC). (A) L1 before the first therapy; (B) hepatobiliary phase L1 before the second therapy; (C) L2 before the first therapy; (D) hepatobiliary phase L2 before the second therapy. The diameter of L2 decreased from 1.63 cm (C) to 1.43 cm (D) (decrease of 12%) after the first therapy.

4. Discussion

It is proven that in rare circumstances, radiation not only directly affects the treated lesions, killing the tumor cells, but can also indirectly modulate the immune infiltration in distant lesions present in the same organ, inducing a positive abscopal effect with a reduction of the lesion. The aim of the study was to investigate the effect that radiation therapy has on lymphocyte infiltration in adjacent, yet untreated lesions, and to evaluate how such an infiltration can affect clinical outcome in patients diagnosed with liver cancer.

4.1 An immunosuppressive tumor microenvironment within the tissue

In this study, the results, analyzing tissue samples from patients with primary and secondary liver cancer, showed an average immune depletion in more than half of the cohort after in-depth immunophenotyping of TILs subgroups. The underlying mechanism behind the change in immune signature remains complicated and largely unknown. It is assumed that this phenomenon is nurtured by multiple factors. The occurrence of immunodepletion suggests an immunosuppressive tumor microenvironment for most of the patients after receiving radiotherapy (140). To our knowledge, the effect of radiotherapy on the tumor microenvironment is still under discussion. Radiotherapy mediates the release of chemokines and cytokines, modifying the balance between immune-inhibitory or immune-stimulatory effects (141). Under certain circumstances, TME after radiotherapy is characterized by increased infiltration of immunosuppressive cells, which include Tregs, M2 macrophages, MDSCs (Myeloid-derived suppressor cells) and NK cells as well as tolerogenic cytokine cascades such as IL-10 and TGF-ß (142, 143). These elements are responsible for the complexity of an immune-inhibitory TME (141). In addition, the tumor-tolerant microenvironment could also be exacerbated by environmental factors (e.g. the presence of hypoxia, pH) after radiotherapy (144). We hypothesize that in our cohort, radiotherapy contributes to an immune-suppressive environment where the functionality and density of immune cells is stamped out by a combination of negative regulators, explaining a later drastic decrease in TILs phenotypes for most patients. At the same time, the immune landscape of individual patients has distinct features with relevant heterogeneity as an increased immune infiltration in several cases was also observed.

4.2 The role of time frame with regard to treatment regimen

We also found that only one CRCLM patient whose time window between two therapies was shorter than 10 days experienced an increased infiltration in all TILs subtypes after radiotherapy, despite the tendency for an immunodepletion seen in the rest of the cohort. Meanwhile, it is also worth mentioning that this patient happened to be the single case in the study whose time frame was less than 10 days. The rest of patients, experienced either a reduction in TILs count or a mixed rise and fall for the five markers. This particular case may be an indicator that the peak for immune infiltration might appear much earlier, possibly immediately after the first radiotherapy. In addition, we could hypothesize that if the second therapy is induced at a later time point where the peak of immune infiltration has passed and the antitumor response is weaker, the probability of detecting a positive abscopal effect is much lower. This assumption is supported by several reported cases that show that the peak of immune infiltration, such as $FOXP3^+$ and $CD8^+$ T cells, emerges within 10 days after the radiotherapy is first induced (145, 146). Nevertheless, relevant experiments were mostly performed on animal models (mice) and very few data from clinical studies on humans is available so far.

To validate this hypothesis on humans, a study with a larger patient cohort and a shift of the observational window between the two therapy sessions within the range of three to five days would be necessary. In this setting, patients may show a higher degree of immune infiltration after the first therapy instead of an immunodepletion. However, one CRCLM patient in our cohort demonstrated an immune spike with a 13-day interval. Meanwhile, a study investigating HCC patients who underwent ^{90}Y radioembolisation revealed that an immune activation including an increase in the number of TILs, was observed both 1 month and 3 months post-therapy (147). Despite focused solely on primary liver cancer, this finding suggested that an immune boost could appear at a much later time point (possibly beyond a 10-day interval). As a consequence, these two cases put the role of time frame in the backdrop of clinical settings even more into question. So far, the rationale behind this remains undetermined. We cannot rule out the possibility that an immune boost still exists after radiotherapy, even if in most cases the peak could be dampened by other immunosuppressive factors, such as presence of macrophages and monocytes in the tumor microenvironment. The number of cases in our cohort is too limited to reach definite

conclusions in this context. More evidence needs to be gathered in order to fully comprehend the role of time frame among different tumor entities.

4.3 The effect of chemotherapy

In addition, patient history before they received radiotherapy was also reviewed. Most patients in our cohort received pre-treatment (chemotherapy, immunotherapy, hormone therapy or even previous radiotherapy sessions) before they were recruited. Of note, most of them were treated with chemotherapy within less than 8 months before they were included in our study. It is widely acknowledged that after chemotherapy, patients are expected to experience a wide spectrum of immunosuppression, especially for $CD8^+$ T cells, $CD4^+$ T cells, and B cells (148). The short-term and long-term effects of chemotherapy on the immune system are largely influenced by the regime of chemotherapy and the response of individuals who receive the therapy. However, in an observational study published by Verma et al (149), it is demonstrated that the compromise of a patient's immune system could last up to 9 months post-therapy. Although this study only focused on breast cancer patients, it still gives a glimpse of how the immune landscape could be altered by chemotherapy in the long-run. In particular, it is stated that B cells and $CD4^+$ T cells experienced a dramatic depletion after chemotherapy. Furthermore, it's shown that the level of B cells and T cells was still not comparable to a pre-treatment level even after nine months of recovery. In light of the limited number of treatment-naïve patients in our study, it is almost impossible to exclude the game-changing role of chemotherapy before the investigation of targeted radiotherapeutic effects. Chemotherapy can be a potential contributing factor to the dysfunction and depletion of lymphocytes. However, it is established that in a clinical setting, most liver malignancies, especially CRCLM, undergo two or more rounds of chemotherapy before radiotherapy, which serves as a standard treatment. (22)

4.4 Possible mechanism behind immunodepletion

Our data showed an elevated expression level of Tim3 positive tumor cells in L2 compared to L1. A substantial decrease was observed in the number of PD-L1 positive tumor cells after radiotherapy. At the same time, we found that a higher amount of PD-1 positive cells in TME correlated to longer overall survival. Overexpression of immune exhaustion markers in the tumor microenvironment, such as PD1, PD-L1 and Tim3, is shown to be the

major cause of physical death of T cells. This could probably explain the rationale behind the observed immune depletion in most cases.

In healthy individuals, moderate levels of inhibitory molecules like PD-1 and its ligands exist as a defense mechanism. Upon the activation of T cells, PD-1 and PD-L1 are upregulated to avoid autoimmunity and maintain hemostasis (150). Evidence has shown that overexpression of T cell exhaustion markers hinders immune response and promotes the progression of cancer (151). Therefore, immunotherapy, such as anti PD-1/PD-L1 inhibitors, has been extensively deployed to disrupt T cell exhaustion, block tumor evasion and subsequently eliminate tumor cells. Immunotherapy proved to be clinically effective in a broad range of malignancies and serve as one of the most successful checkpoint inhibitors (152). Based on our hypothesis, an upregulation of PD-L1 on tumor cells or an upregulation of PD-1 on immune cells from L1 to L2 could be expected. Surprisingly, in our cohort, most patients displayed a substantial downregulation of PD-L1 positive tumor cells after radiotherapy. Meanwhile, very little expression of PD-1 in TME was observed (around 1~2%). Most of the cases also did not show a significant change of PD-1 expression, indicating that our hypothesis with regard to PD-L1/PD-1 is in contradiction to the results. It also suggests that the PD-L1/PD-1 pathway is at least not the only pathway to account for the decline of TILs in most cases. This has been confirmed by the marginal efficacy of PD-1/PD-L1 inhibitors in liver metastasis due to their limited expression (153). Although radiotherapy in combination with PD-1/PD-L1 inhibitors proved to prompt the anti-tumor response of the immune system, it still holds true that based on the feature of a specific tumor microenvironment, combining RT with other pathway checkpoint blockades could have higher efficiency in clinical practice.

Moreover, an increased expression level of Tim3 after radiotherapy may indicate its crucial role in the tumor microenvironment. Tim3, an emerging co-inhibitory receptor, has been increasingly seen as a novel candidate involved in immunotherapy. Although no significant correlation with regard to OS was revealed in our cohort, largely due to the small cohort size, the controversial role of Tim3 is still worth noticing. Findings concerning the prognostic value of Tim3 hugely differ when various tumor entities and other clinical parameters were taken into consideration (154, 155). Tim3 is reported to act as a negative regulator and unfavorable prognostic marker in a range of cancers, including HCC and colon cancer (123,

156). On the contrary, especially in renal carcinoma (157, 158), patients with a higher number of Tim3 positive tumor cells are shown to have a better clinical outcome. Despite prognostic relevance revealed in a range of studies (159, 160), the function and molecular signaling mechanism of Tim3 has not been fully elucidated.

In addition, a positive prognostic value of PD-1 in TME was discovered in our study. Nevertheless, the prognostic role of PD-1 is still under controversy. Studies showed that for example, in breast, renal cell cancer or CRC, a favorable prognostic significance of PD-1 is in line with our finding (161-163). However, even in the same type of cancer, such as CRC, the role of PD-1 as a negative prognostic marker has also been reported (122, 164, 165). Furthermore, evidence has been accumulated that co-expression of multiple cell surface inhibitory molecules is a critical and most indicative feature of exhausted T cells rather than expression of an individual marker. All of these Immune cell co-inhibitory receptors, such as PD-1/PD-L1, CTLA-4, LAG3 (lymphocyte activation gene 3 protein), TIGIT (T cell immunoreceptor with Ig and ITIM domain) and Tim3 are implicated in regulating the exhaustion of T cells and therefore dampen host immune response to cancer (106) (figure 22). This could partly explain that results solely concerning PD-1/PD-L1 or Tim3 were not adequate to support our theory of immune depletion. In this regard, combined blockades of multiple molecular pathways could maximize its efficacy in restoring the functionality of T cells (151). In the future, it would be of great interest to further explore other types of immune inhibitors for a deep understanding of the immune microenvironment.

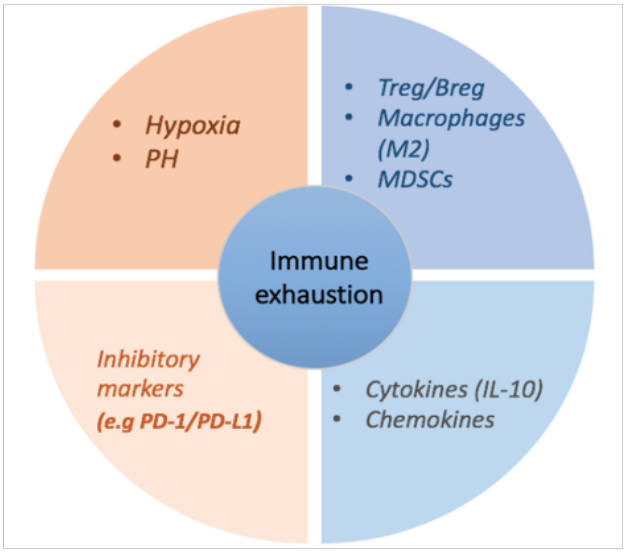

Figure 21. The contributing factors of immune exhaustion. The phenomenon of immune exhaustion is complicated by existence of environmental factors (e.g. pH, hypoxia), upregulation of inhibitory markers (e.g. PD-1/PD-L1), and release of immunosuppressive cytokines (e.g. IL-10) as well as the surge in regulatory cells (e.g. Tregs/ Bregs).

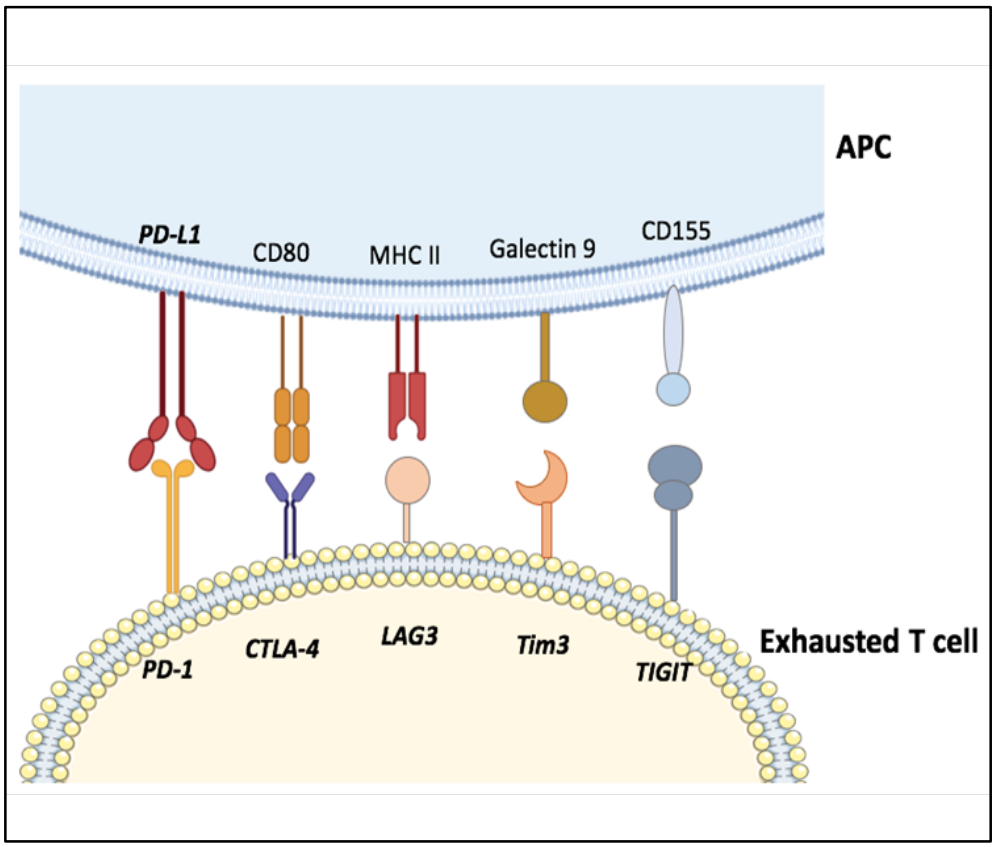

Figure 22. The expression of immune exhaustion markers. The co-expression of surface receptors on T cells is a cardinal feature of exhausted T cells. The degree of immune exhaustion largely depends upon the expression level as well as the types of exhaustion markers.

4.5 Infiltration pattern of TILs

Representative regions of interest demonstrated that in a few observed cases of liver metastasis immune infiltrates were mainly clustered in the invasive margin of peri- or intra-tumoral areas while nearly absent in the core tumor region. By contrast, in HCC, a distinct distribution pattern of extensive infiltrates was noted in both IM and CT regions. These findings were also consistent with what was revealed in other studies, for example, it has been shown that in secondary lesion sites, immune density is higher in the invasive margin than in the tumor center (166). Besides, Halama et al. found that in the invasive margin in patients with colorectal cancer liver metastasis, immune cells are even exclusively present in the invasive margin (71). Interestingly, studies have also suggested

that in metastasis, the distribution of immune infiltrates is ordinarily mirroring the one in the primary lesion. Yet, immune infiltration in metastases is weaker than that in a primary lesion (167). Importantly, growing evidence provides support that primary liver cancer (HCC), an immunogenic tumor, is commonly abundantly infiltrated with lymphocyte infiltrates, including CD8 and Tregs (168). Nevertheless, the mechanism behind this observation is not well understood yet. We hypothesize that the dense and compact structure of metastasis itself possibly contributes to the lower immune cell infiltration in secondary tumor sites. Compared to the relatively loose structure of a primary tumor, the solid tumoral structure of metastatic sites may hamper immune cell infiltrates to reach the core region of a lesion. Furthermore, metastatic cells may exhibit increased immune resistance after escaping from the immune reaction in primary malignant sites (169). Hence, it adds extra difficulty for penetration of TILs into the tumor center and leads to a notoriously poor response to immunotherapy. This hypothesis also needs validation by future studies.

4.6 Prognostic value of TILs

We found that patients with a higher count of $CD20^+$ B cells in L2 tend to have a shorter overall survival. Nevertheless, the role of $CD20^+$ B cells in the TME still remains unclear. Even though a favorable prognostic value of $CD20^+$ B cells was indicated in more than half of relevant studies (170), evidence has surfaced that $CD20^+$ B cells can also have a negative effect in the immune microenvironment (171). In recent years, regulatory B cells (Bregs), an important subtype of B cells, have been found to be commonly involved in cancer progression. Bregs are capable of impairing the activation of T cells by producing anti-inflammatory factors (IL-10, etc.), thus negatively regulating or suppressing anti-tumor immune response (172). However, to date no clear definition and classification of Bregs has been agreed upon (173), nor specific markers for Bregs have been identified (174). Hence, the qualification and quantification of Bregs remain as an unsolved challenge. Here, we hypothesize that the negative correlation obtained between $CD20^+$ B cells and clinical outcome is attributable by the presence of large amounts of $CD20^+$ regulatory B cells in TME after radiotherapy. It is presumed that radiotherapy triggers the shift from regular $CD20^+$ B cells toward the differentiation of regulatory $CD20^+$ B cells, which could explain the negative prognostic value of $CD20^+$ B cells revealed in our study. Nevertheless, the mechanistic reasoning behind it remains elusive and still needs further proof (172).

A negative prognostic role of CD20/CD8 ratio was also discovered in our group. To our knowledge, the notion of CD20/CD8 ratio has been referred to scarcely, therefore further investigations are required to validate our results. Although in one study, it was confirmed that a higher T and B cell score (CD8/CD20) in colorectal cancer patients is associated with a longer overall survival (175). This was concordant with our finding regarding CD20/CD8 ratio. We also found that patients with a higher CD4/CD45RO ratio tend to have worse clinical outcomes. On the contrary, a high CD8/CD45RO ratio was associated with a longer survival. Overall, very few studies were carried out regarding the clinical value of CD4/CD45RO or CD8/CD45RO ratio. Due to discrepancies in the feature of the tumor microenvironment, the antitumor trait of $CD8^+$ T cells is extensively acknowledged while the prognostic value of CD4 is still controversial (176-178). In addition, it has been proven that CD45RO serves as a favorable prognostic marker in a wide range of solid tumors (179). As a memory T cell marker, $CD45RO^+$ T cells (mostly $CD4^+CD45RO^+$ T cells and $CD8^+CD45RO^+$ T cells) are differentiated from naïve $CD4^+$ or $CD8^+$ cells after they encounter foreign antigens in order to prepare for future immune responses (87). However, aforementioned CD4/CD45, CD8/CD45 or CD20/CD8 ratio were shown to have a weak correlation to OS ($0.05<p\text{-value}<0.1$). The borderline significance we observed was largely due to the small cohort size and heterogeneity of patients in our study. Although our results require further validation, this finding can nevertheless provide some clue about the relationship between distinct markers. In light of the heterogeneity in terms of tumor entity in our cohort, it is challenging to elaborate an immunoscore which can be applicable to all patients. Nevertheless, these results could serve as a basis for constructing a future immunoscore once more data is available.

4.7 Investigation of a possible abscopal effect

No case of positive abscopal effect was discovered in our small cohort. We found that one HCC patient showed a small decrease in the size of the distal lesion. However, being less than 30% in reduction, this change did not qualify for a Partial Response (PR). As it has been reported, most clinical cases of abscopal effect are more likely to appear in tumors with high immunogenicity, such as melanoma (180). It is therefore plausible that a slight shrinkage was observed in an HCC patient given the fact that HCC is an immunogenic tumor type as well (181, 182). The rest of the cohort displayed either growth or a minimal change distant to the treated site. For cases where a narrow change was seen in the size of

the untreated lesion, one can assume that either the time frame in between two therapy sessions was too short for any change to be detected or the force of tumor-attacking immune cells and malignant cancer cells is more or less in equilibrium. It is also revealed in multiple studies that a positive abscopal effect is an extremely rare occurrence when radiotherapy is induced alone. Also, only 46 well-documented clinical cases of abscopal effect have been reported in the period of 1969 and 2014. A retrospective study investigating patients with hepatic metastases who received radioembolization recently showed that only one positive abscopal effect was identified out of 907 originally investigated cases (183). In view of the small number of patients ultimately included in our observation, great care is needed when it comes to the identification of a possible abscopal effect. The rarity of this event can be expected as immune cells induced via radiotherapy have to overcome a strong immunosuppressive barrier in order to elicit a robust systemic immune response or even a positive abscopal effect in untreated lesions (35). Furthermore, probability of a positive abscopal effect is much higher when radiotherapy is combination with immunotherapy as it is validated by other studies (38, 184, 185). In this circumstance, lymphocytes are more likely to be primed and activated to override the immune-suppressive nature of the tumor microenvironment through the synergistic anti-tumor effects of radiation and immunotherapy (immune checkpoint inhibitors).

4.8 Limitations

The limitations of this retrospective study are mostly contributed by the small cohort size as well as the heterogeneity of our patients. The main goal of our explorative study was to provide a general outlook of the immune profile beyond different cancer types, to explore an optimal therapy regime and add clues for the establishment of a potential immune pattern. This also explains the variability in time interval between therapy sessions in our study. These factors greatly accounted for the strenuous interpretation of results. With respect to the occurence of a possible abscopal effect, MRI images of recruited patients at two time points (shortly before 1st and 2nd radiotherapy) were examined. However, only a few patients met the recruiting requirements whereas the imaging data of most recruited patients were irretrievable. This also adds to the difficulty in the investigation of the abscopal effect. In future-related studies, well-written records concerning characteristics of the investigated lesion and documentation of imaging data need be taken into account. Although we hypothesized that the immune landscape of two distant lesions before the first therapy should be histologically comparable, there is still a chance that they could be highly divergent. In addition, the localization in the organ (intra-tumoral, peri-tumoral or stroma area) where a biopsy sample was taken also greatly affects our evaluation and interpretation of the results.

4.9 Future direction and perspectives

Our study is unique in two aspects: 1) we attempted to examine the value of TILs across a variety of cancer types. 2) This is one of the very few studies that sought to explore a possible existence of positive abscopal effect in a clinical setting. To further interrogate the immune microenvironment through the immunophenotyping, a larger cohort composed of a more homogeneous group of patients is urgently required. The role of the time interval between two therapy sessions remains largely unclarified, therefore it is essential to establish an optimal time interval based on cell or animal models before therapy regimes are deployed on humans. Also, the evaluation of multiple immune inhibitor markers is needed to elucidate the complex interplay between various components in the tumor microenvironment. The tumor microenvironment is a complicated and dynamic network of cellular and molecular elements. Consequently, investigation of the expression level of macrophages (CD68, CD86, and CD163), a T cell marker (CD3) as well as other potential

markers could shed some light to the makeup and dynamics of the examined tumor microenvironment. A more complete and comprehensive immune profile can therefore be established for navigation of personalized treatment and individualized medicine.

Eventually, the phenomenon of immune depletion present in most cases as well as the results concerning the prognostic value of TILs are a reflection of a mixture of confounders. Hence, a precise assessment of the tumor microenvironment is challenging in our study. Importantly, biopsy samples are a static snapshot reflecting the proportional components of the tumor microenvironment at time points where certain TILs subgroups are more dominant than others. The role of an individual cellular type is in constant development along the timeline in the progression of the disease. Therefore, biopsy samples in combination with other examination methods (e.g. miRNAs) could bring a clearer picture of the complex immune landscape. Liver cancer, especially liver metastasis, is notoriously difficult to treat. Therefore, the positive abscopal effect, a systemic response inducing the shrinkage in a distal and untreated lesion, has significant and profound clinical implications. However, as a rare clinical event shown in both literature and our study, the underlying rationale for this phenomenon requires further investigation in order to establish a possible pattern or method with repeatability and reproducibility.

5. Conclusion

In the present study, an average immune depletion was observed for TILs subpopulations after radiotherapy. In addition, evidence is provided that $CD20^{+}$ B cells acted as an independent prognostic marker while ratios based on CD8/CD45, CD20/CD8 and CD4/CD45 also had prognostic value with regard to overall survival. Although our study is exploratory, it strongly suggests that analysis of tissue samples, particularly regarding TILs, could help create an immune profile to assist stratification of patients for therapy. This study also points towards future studies based on a larger and more comprehensive cohort with fewer variables in therapy regime, offering novel guidance for interventional strategies in personalized combined treatment regimes.

6. Summary

Background: Liver cancer is a highly heterogeneous malignant disease. Radiotherapy is a treatment eligible for patients with liver cancer who are at advanced stages and not suited for curative treatments such as liver transplantation or surgical resection. However, in the light of high mortality rates for liver cancer and frequent recurrence or progression after radiotherapy, it remains relevant for oncologists and radiologists to adjust the treatment regime longitudinally. It is proven that under rare circumstances, a positive abscopal effect can be induced after radiotherapy, therefore leading to the regression of distant, untreated lesions and bringing survival benefits to patients. Our study aimed to investigate the effect of radiotherapy on the dynamic changes of TILs in adjacent, untreated lesions and explore the prognostic value.

Methods: n=21 primary and secondary liver cancer patients were retrospectively recruited into the study from the AROMA and THIAMAT study format. Biopsy samples (n=42) were available from two distant lesions at two different time points (pre-1st therapy in irradiated lobe and pre-2nd therapy in non-irradiated lobe). Tissue samples were processed by a multiplex immunophenotyping approach featuring a panel of immune markers (CD4, CD8, CD20, CD45RO and FoxP3). TILs in liver tissues were qualitatively and quantitatively assessed at both lesions accordingly. Prognostic value of single cell markers and ratios based on two markers were investigated. We also compared infiltration patterns within the tissue in HCC and liver metastasis. Furthermore, immune exhaustion markers were also examined and quantified using immunohistochemistry analysis.

Results: In our study, an average decrease in the number of TILs was observed after the first radiotherapy. Additionally, in liver metastasis, immune infiltrates were mostly observed in the invasive margin of peri-tumoral and intra-tumoral areas while absent in the core region. CD20, CD4/CD45, CD20/CD8 and CD8/CD45 showed the most significant outcomes. A high density of CD20^{+} B cells were inversely associated with a worse clinical outcome ($p=0.048$). Also, a borderline significance was found between ratios and overall survival. A higher CD4/CD45 ($p=0.068$) and CD20/CD8 ($p=0.080$) were seen to have a negative effect on survival rate. A higher CD8/CD45 ($p=0.093$) ratio was associated with longer survival.

Conclusions: Under certain circumstances, radiation therapy was proven to lead to a depletion of TILs in the tumor microenvironment. Multiple factors, including an immune-suppressive TME, a prolonged time window in between therapy sessions, an inducement of previous chemotherapies and an over-expression of immune exhaustion

markers (Tim3, PD-L1/PD-1 pathway), could potentially contribute to this phenomenon. However, any individual element among them was found not entirely responsible for immunodepletion. $CD20^+$ B cells as well as CD8/CD45, CD20/CD8 and CD4/CD45 ratios are considered independent predictors of overall survival. Furthermore, the therapeutic stimulus of radiotherapy alone remains insufficient to evoke a positive abscopal effect. A combination of radiotherapy and immunotherapy may serve as a potential strategy to increase pro-immunogenic response. In the future, our experiments could help to provide clues for clinical evaluation of patients, thus contributing to stratification of patients for individualized therapy.

7. Zusammenfassung

Hintergrund: Primäre und sekundäre Lebermalignome sind eine heterogene Gruppe von Tumoren, bei denen im fortgeschrittenen Stadium die Strahlentherapie eine wichtige Rolle spielt, wenn kurative Behandlungsansätze wie eine chirurgische Resektion oder Lebertransplantation nicht in Frage kommen. Angesichts der hohen Sterblichkeitsrate bei Lebertumoren und des häufigen Wiederauftretens oder Fortschreitens nach einer Strahlentherapie, ist es äußerst wichtig, das Behandlungsregime so gut wie möglich zu gestalten und anzupassen. Es ist erwiesen, dass in seltenen Fällen nach einer Strahlentherapie ein positiver abskopaler Effekt auftreten kann, der zu einer Schrumpfung entfernter, unbehandelter Läsionen führt und den Patienten einen Überlebensvorteil verschafft. Ziel unserer Studie ist die Untersuchung der Auswirkungen der Strahlentherapie auf die dynamischen Veränderungen der TILs in benachbarten, unbehandelten Läsionen und die Ermittlung ihrer prognostischen Aussagekraft.

Methoden: n=21 Patienten mit primären und sekundären Lebertumoren wurde retrospektiv aus den AROMA und THIAMAT Studienpatienten für die Studie rekrutiert. Biopsieproben (n=42) der Patienten standen von zwei Läsionen zu zwei verschiedenen Zeitpunkten zu Verfügung (vor der ersten Therapie im bestrahlten Lappen und vor der zweiten Therapie im nicht bestrahlten Lappen). Die Gewebeproben wurden mit Multiplex-Immunphänotypisierung auf Immunmarker (CD4, CD8, CD20, CD45RO und FoxP3) gefärbt. Die TILs im Lebergewebe wurden qualitativ und quantitativ erfasst. Die prognostische Aussagekraft einzelner Zellmarker und die des Quotienten zweier Marker wurden untersucht. Außerdem wurde das Infiltrationsmuster innerhalb des Gewebes beim Hepatocellulären Karzinom und Lebermetastasen untersucht. Darüber hinaus wurden Marker der Erschöpfung des Immunsystems mit immunhistochemischer Analyse untersucht und quantifiziert.

Ergebnisse: In unserer Studie wurde ein Rückgang der Anzahl der TILs nach der ersten Strahlentherapie festgestellt. Darüber hinaus wurden bei Lebermetastasen Immuninfiltrate hauptsächlich am invasiven Rand der peri-tumoralen und intra-tumoralen Bereiche beobachtet, während sie in den zentralen Tumoranteilen fehlten. CD20, CD4/CD45, CD20/CD8 und CD8/CD45 zeigten die signifikantesten Ergebnisse. Die Dichte der $CD20^{+}$ B-Zellen zeigte eine inverse Korrelation mit dem klinischen Outcome (p=0,048). Eine grenzwertige Signifikanz wurde zwischen den Quotienten und dem Gesamtüberleben festgestellt. Ein höherer Quotient aus CD4/CD45 (p=0,068) und CD20/CD8 (p=0,080) wirkte

sich negativ auf die Überlebenswahrscheinlichkeit aus. Ein höheres CD8/CD45-Verhältnis (p=0,093) wurde mit einem längeren Überleben in Verbindung gebracht.

Schlussfolgerungen: Die Strahlentherapie führt zu einer signifikanten Verminderung der TILs im Mikromilieu des Tumors. Mehrere Faktoren, darunter eine immunsuppressive Tumormikroumgebung, ein langes Zeitintervall zwischen den Therapien, eine Induktion durch vorangegangene Chemotherapie und eine Überexpression von Markern der Erschöpfung des Immunsystems (Tim3, PD-L1/PD-1-Signalweg), könnten wesentlich zu diesem Phänomen beitragen. Es hat sich jedoch gezeigt, dass kein einzelnes Element allein für die Immunerschöpfung verantwortlich ist. $CD20^+$ B-Zellen sowie das Verhältnis von CD8/CD45, CD20/CD8 und CD4/CD45 gelten als unabhängige Prädiktoren für das Gesamtüberleben. Darüber hinaus reicht die alleinige Durchführung einer Strahlentherapie nicht aus, um einen positiven abskopalen Effekt hervorzurufen. Eine Kombination aus Strahlentherapie und Immuntherapie könnte bessere Ergebnisse erzielen. In Zukunft könnten unsere Experimente dazu beitragen, Anhaltspunkte für die klinische Bewertung von Patienten zu liefern, und damit einen Beitrag zur Stratifizierung von Patienten für eine individualisierte Therapie leisten.

8. References

1. Ferlay J, Soerjomataram I, Dikshit R, Eser S, Mathers C, Rebelo M, et al. Cancer incidence and mortality worldwide: sources, methods and major patterns in GLOBOCAN 2012. International journal of cancer. 2015;136(5):E359-86.

2. Bruix J, Cheng AL, Meinhardt G, Nakajima K, De Sanctis Y, Llovet J. Prognostic factors and predictors of sorafenib benefit in patients with hepatocellular carcinoma: Analysis of two phase III studies. Journal of hepatology. 2017;67(5):999-1008.

3. Kim DW, Talati C, Kim R. Hepatocellular carcinoma (HCC): beyond sorafenib-chemotherapy. Journal of gastrointestinal oncology. 2017;8(2):256-65.

4. Petrick JL, McGlynn KA. The changing epidemiology of primary liver cancer. Curr Epidemiol Rep. 2019;6(2):104-11.

5. Gomaa AI, Khan SA, Toledano MB, Waked I, Taylor-Robinson SD. Hepatocellular carcinoma: epidemiology, risk factors and pathogenesis. World J Gastroenterol. 2008;14(27):4300-8.

6. Dragani TA. Risk of HCC: genetic heterogeneity and complex genetics. J Hepatol. 2010;52(2):252-7.

7. Simard EP, Ward EM, Siegel R, Jemal A. Cancers with increasing incidence trends in the United States: 1999 through 2008. CA: a cancer journal for clinicians. 2012;62(2):118-28.

8. Adam R, De Gramont A, Figueras J, Guthrie A, Kokudo N, Kunstlinger F, et al. The oncosurgery approach to managing liver metastases from colorectal cancer: a multidisciplinary international consensus. Oncologist. 2012;17(10):1225-39.

9. Hackl C, Neumann P, Gerken M, Loss M, Klinkhammer-Schalke M, Schlitt HJ. Treatment of colorectal liver metastases in Germany: a ten-year population-based analysis of 5772 cases of primary colorectal adenocarcinoma. BMC Cancer. 2014;14:810.

10. Manfredi S, Lepage C, Hatem C, Coatmeur O, Faivre J, Bouvier AM. Epidemiology and management of liver metastases from colorectal cancer. Annals of surgery. 2006;244(2):254-9.

11. Engstrand J, Nilsson H, Stromberg C, Jonas E, Freedman J. Colorectal cancer liver metastases - a population-based study on incidence, management and survival. BMC Cancer. 2018;18(1):78.

12. House MG, Ito H, Gonen M, Fong Y, Allen PJ, DeMatteo RP, et al. Survival after hepatic resection for metastatic colorectal cancer: trends in outcomes for 1,600 patients during two

decades at a single institution. Journal of the American College of Surgeons. 2010;210(5):744-52, 52-5.

13. Roxburgh P, Evans TR. Systemic therapy of hepatocellular carcinoma: are we making progress? Adv Ther. 2008;25(11):1089-104.

14. Baskar R, Lee KA, Yeo R, Yeoh KW. Cancer and radiation therapy: current advances and future directions. International journal of medical sciences. 2012;9(3):193-9.

15. Sundram FX, Buscombe JR. Selective internal radiation therapy for liver tumours. Clinical medicine (London, England). 2017;17(5):449-53.

16. Forstner DF, Yap ML. Advances in radiation therapy. The Medical journal of Australia. 2015;203(10):394-5.

17. Abshire D, Lang MK. The Evolution of Radiation Therapy in Treating Cancer. Seminars in oncology nursing. 2018;34(2):151-7.

18. Ricke J, Wust P, Stohlmann A, Beck A, Cho CH, Pech M, et al. CT-guided interstitial brachytherapy of liver malignancies alone or in combination with thermal ablation: phase I-II results of a novel technique. Int J Radiat Oncol Biol Phys. 2004;58(5):1496-505.

19. Ricke J, Wust P, Wieners G, Beck A, Cho CH, Seidensticker M, et al. Liver malignancies: CT-guided interstitial brachytherapy in patients with unfavorable lesions for thermal ablation. J Vasc Interv Radiol. 2004;15(11):1279-86.

20. Zaorsky NG, Davis BJ, Nguyen PL, Showalter TN, Hoskin PJ, Yoshioka Y, et al. The evolution of brachytherapy for prostate cancer. Nature reviews Urology. 2017;14(7):415-39.

21. Bretschneider T, Ricke J, Gebauer B, Streitparth F. Image-guided high-dose-rate brachytherapy of malignancies in various inner organs - technique, indications, and perspectives. J Contemp Brachytherapy. 2016;8(3):251-61.

22. Kennedy A. Radioembolization of hepatic tumors. J Gastrointest Oncol. 2014;5(3):178-89.

23. Kallini JR, Gabr A, Salem R, Lewandowski RJ. Transarterial Radioembolization with Yttrium-90 for the Treatment of Hepatocellular Carcinoma. Adv Ther. 2016;33(5):699-714.

24. Narsinh KH, Cui J, Papadatos D, Sirlin CB, Santillan CS. Hepatocarcinogenesis and LI-RADS. Abdominal radiology (New York). 2018;43(1):158-68.

25. Sangro B, Inarrairaegui M, Bilbao JI. Radioembolization for hepatocellular carcinoma. Journal of hepatology. 2012;56(2):464-73.

26. Salem R, Gordon AC, Mouli S, Hickey R, Kallini J, Gabr A, et al. Y90 Radioembolization Significantly Prolongs Time to Progression Compared With Chemoembolization in Patients With Hepatocellular Carcinoma. Gastroenterology. 2016;151(6):1155-63.e2.

27. El Fouly A, Ertle J, El Dorry A, Shaker MK, Dechene A, Abdella H, et al. In intermediate stage hepatocellular carcinoma: radioembolization with yttrium 90 or chemoembolization? Liver international : official journal of the International Association for the Study of the Liver. 2015;35(2):627-35.

28. Bester L, Meteling B, Pocock N, Pavlakis N, Chua TC, Saxena A, et al. Radioembolization versus standard care of hepatic metastases: comparative retrospective cohort study of survival outcomes and adverse events in salvage patients. J Vasc Interv Radiol. 2012;23(1):96-105.

29. Seidensticker R, Denecke T, Kraus P, Seidensticker M, Mohnike K, Fahlke J, et al. Matched-pair comparison of radioembolization plus best supportive care versus best supportive care alone for chemotherapy refractory liver-dominant colorectal metastases. Cardiovascular and interventional radiology. 2012;35(5):1066-73.

30. Goin JE, Salem R, Carr BI, Dancey JE, Soulen MC, Geschwind JF, et al. Treatment of unresectable hepatocellular carcinoma with intrahepatic yttrium 90 microspheres: factors associated with liver toxicities. J Vasc Interv Radiol. 2005;16(2 Pt 1):205-13.

31. Deng X, Wu H, Gao F, Su Y, Li Q, Liu S, et al. Brachytherapy in the treatment of breast cancer. International journal of clinical oncology. 2017;22(4):641-50.

32. Raval M, Bande D, Pillai AK, Blaszkowsky LS, Ganguli S, Beg MS, et al. Yttrium-90 radioembolization of hepatic metastases from colorectal cancer. Front Oncol. 2014;4:120.

33. Leung S, Sexton M. Radical radiation therapy for carcinoma of the vagina--impact of treatment modalities on outcome: Peter MacCallum Cancer Institute experience 1970-1990. Int J Radiat Oncol Biol Phys. 1993;25(3):413-8.

34. Schnapauff D, Collettini F, Hartwig K, Wieners G, Chopra S, Hamm B, et al. CT-guided brachytherapy as salvage therapy for intrahepatic recurrence of HCC after surgical resection. Anticancer research. 2015;35(1):319-23.

35. Rodriguez-Ruiz ME, Vanpouille-Box C, Melero I, Formenti SC, Demaria S. Immunological Mechanisms Responsible for Radiation-Induced Abscopal Effect. Trends in immunology. 2018;39(8):644-55.

36. Erinjeri JP, Fine GC, Adema GJ, Ahmed M, Chapiro J, den Brok M, et al. Immunotherapy and the Interventional Oncologist: Challenges and Opportunities-A Society of Interventional Oncology White Paper. Radiology. 2019;292(1):25-34.

37. Ngwa W, Irabor OC, Schoenfeld JD, Hesser J, Demaria S, Formenti SC. Using immunotherapy to boost the abscopal effect. Nature reviews Cancer. 2018;18(5):313-22.

38. Reynders K, Illidge T, Siva S, Chang JY, De Ruysscher D. The abscopal effect of local radiotherapy: using immunotherapy to make a rare event clinically relevant. Cancer treatment reviews. 2015;41(6):503-10.

39. Salama AK, Postow MA, Salama JK. Irradiation and immunotherapy: From concept to the clinic. Cancer. 2016;122(11):1659-71.

40. Ohba K, Omagari K, Nakamura T, Ikuno N, Saeki S, Matsuo I, et al. Abscopal regression of hepatocellular carcinoma after radiotherapy for bone metastasis. Gut. 1998;43(4):575-7.

41. Postow MA, Callahan MK, Barker CA, Yamada Y, Yuan J, Kitano S, et al. Immunologic correlates of the abscopal effect in a patient with melanoma. The New England journal of medicine. 2012;366(10):925-31.

42. Hu ZI, McArthur HL, Ho AY. The Abscopal Effect of Radiation Therapy: What Is It and How Can We Use It in Breast Cancer? Current breast cancer reports. 2017;9(1):45-51.

43. Eggert T, Greten TF. Tumor regulation of the tissue environment in the liver. Pharmacology & therapeutics. 2017;173:47-57.

44. Demaria S, Golden EB, Formenti SC. Role of Local Radiation Therapy in Cancer Immunotherapy. JAMA oncology. 2015;1(9):1325-32.

45. Erinjeri JP, Thomas CT, Samoilia A, Fleisher M, Gonen M, Sofocleous CT, et al. Image-guided thermal ablation of tumors increases the plasma level of interleukin-6 and interleukin-10. J Vasc Interv Radiol. 2013;24(8):1105-12.

46. Tanis E, Nordlinger B, Mauer M, Sorbye H, van Coevorden F, Gruenberger T, et al. Local recurrence rates after radiofrequency ablation or resection of colorectal liver metastases. Analysis of the European Organisation for Research and Treatment of Cancer #40004 and #40983. European journal of cancer (Oxford, England : 1990). 2014;50(5):912-9.

47. Sun L, Wang X, Saredy J, Yuan Z, Yang X, Wang H. Innate-adaptive immunity interplay and redox regulation in immune response. Redox biology. 2020;37:101759.

48. Bonilla FA, Oettgen HC. Adaptive immunity. The Journal of allergy and clinical immunology. 2010;125(2 Suppl 2):S33-40.

49. Beutler B. Innate immunity: an overview. Molecular immunology. 2004;40(12):845-59.

50. Kamradt T, Ferrari-Kühne K. [Adaptive immunity]. Deutsche medizinische Wochenschrift (1946). 2011;136(33):1678-83.

51. Santoiemma PP, Powell DJ, Jr. Tumor infiltrating lymphocytes in ovarian cancer. Cancer biology & therapy. 2015;16(6):807-20.

52. Solinas C, Carbognin L, De Silva P, Criscitiello C, Lambertini M. Tumor-infiltrating lymphocytes in breast cancer according to tumor subtype: Current state of the art. Breast (Edinburgh, Scotland). 2017;35:142-50.

53. Ding W, Xu X, Qian Y, Xue W, Wang Y, Du J, et al. Prognostic value of tumor-infiltrating lymphocytes in hepatocellular carcinoma: A meta-analysis. Medicine. 2018;97(50):e13301.

54. Shibutani M, Maeda K, Nagahara H, Fukuoka T, Iseki Y, Matsutani S, et al. Tumor-infiltrating Lymphocytes Predict the Chemotherapeutic Outcomes in Patients with Stage IV Colorectal Cancer. In vivo (Athens, Greece). 2018;32(1):151-8.

55. Portella L, Scala S. Ionizing radiation effects on the tumor microenvironment. Semin Oncol. 2019;46(3):254-60.

56. Grass GD, Krishna N, Kim S. The immune mechanisms of abscopal effect in radiation therapy. Current problems in cancer. 2016;40(1):10-24.

57. Zhu J, Yamane H, Paul WE. Differentiation of effector CD4 T cell populations (*). Annual review of immunology. 2010;28:445-89.

58. Baumjohann D. Diverse functions of miR-17-92 cluster microRNAs in T helper cells. Cancer Lett. 2018;423:147-52.

59. Haabeth OA, Tveita AA, Fauskanger M, Schjesvold F, Lorvik KB, Hofgaard PO, et al. How Do CD4(+) T Cells Detect and Eliminate Tumor Cells That Either Lack or Express MHC Class II Molecules? Front Immunol. 2014;5:174.

60. Borst J, Ahrends T, Bąbała N, Melief CJM, Kastenmüller W. CD4(+) T cell help in cancer immunology and immunotherapy. Nature reviews Immunology. 2018;18(10):635-47.

61. Rakhra K, Bachireddy P, Zabuawala T, Zeiser R, Xu L, Kopelman A, et al. CD4(+) T cells contribute to the remodeling of the microenvironment required for sustained tumor regression upon oncogene inactivation. Cancer cell. 2010;18(5):485-98.

62. Wang Z, Zhao J, Zhao H, A S, Liu Z, Zhang Y, et al. Infiltrating CD4/CD8 high T cells shows good prognostic impact in pancreatic cancer. International journal of clinical and experimental pathology. 2017;10(8):8820-8.

63. Wang Z, Zhao H, Zhao J, A S, Liu Z, Han T, et al. Prognostic significance of CD4 and interleukin-22 expression in pancreatic cancer. International journal of clinical and experimental pathology. 2017;10(9):9846-52.

64. Fu J, Zhang Z, Zhou L, Qi Z, Xing S, Lv J, et al. Impairment of CD4+ cytotoxic T cells predicts poor survival and high recurrence rates in patients with hepatocellular carcinoma. Hepatology (Baltimore, Md). 2013;58(1):139-49.

65. Katz SC, Pillarisetty V, Bamboat ZM, Shia J, Hedvat C, Gonen M, et al. T cell infiltrate predicts long-term survival following resection of colorectal cancer liver metastases. Annals of surgical oncology. 2009;16(9):2524-30.

66. Yuan CH, Sun XM, Zhu CL, Liu SP, Wu L, Chen H, et al. Amphiregulin activates regulatory T lymphocytes and suppresses CD8+ T cell-mediated anti-tumor response in hepatocellular carcinoma cells. Oncotarget. 2015;6(31):32138-53.

67. Bennett SR, Carbone FR, Karamalis F, Flavell RA, Miller JF, Heath WR. Help for cytotoxic-T-cell responses is mediated by CD40 signalling. Nature. 1998;393(6684):478-80.

68. Doherty PC, Topham DJ, Tripp RA. Establishment and persistence of virus-specific CD4+ and CD8+ T cell memory. Immunological reviews. 1996;150:23-44.

69. Flores-Mendoza G, Rodríguez-Rodríguez N, Rubio RM, Madera-Salcedo IK, Rosetti F, Crispín JC. Fas/FasL Signaling Regulates CD8 Expression During Exposure to Self-Antigens. Front Immunol. 2021;12:635862.

70. Ye LL, Wei XS, Zhang M, Niu YR, Zhou Q. The Significance of Tumor Necrosis Factor Receptor Type II in CD8(+) Regulatory T Cells and CD8(+) Effector T Cells. Front Immunol. 2018;9:583.

71. Halama N, Michel S, Kloor M, Zoernig I, Benner A, Spille A, et al. Localization and density of immune cells in the invasive margin of human colorectal cancer liver metastases are prognostic for response to chemotherapy. Cancer research. 2011;71(17):5670-7.

72. Gabrielson A, Wu Y, Wang H, Jiang J, Kallakury B, Gatalica Z, et al. Intratumoral CD3 and CD8 T-cell Densities Associated with Relapse-Free Survival in HCC. Cancer Immunol Res. 2016;4(5):419-30.

73. Huang Y, Ma C, Zhang Q, Ye J, Wang F, Zhang Y, et al. CD4+ and CD8+ T cells have opposing roles in breast cancer progression and outcome. Oncotarget. 2015;6(19):17462-78.

74. Zheng X, Song X, Shao Y, Xu B, Chen L, Zhou Q, et al. Prognostic role of tumor-infiltrating lymphocytes in gastric cancer: a meta-analysis. Oncotarget. 2017;8(34):57386-98.

75. Fridman WH, Pages F, Sautes-Fridman C, Galon J. The immune contexture in human tumours: impact on clinical outcome. Nat Rev Cancer. 2012;12(4):298-306.

76. Sakaguchi S, Miyara M, Costantino CM, Hafler DA. FOXP3+ regulatory T cells in the human immune system. Nature reviews Immunology. 2010;10(7):490-500.

77. Nakamura K, Kitani A, Strober W. Cell contact-dependent immunosuppression by CD4(+)CD25(+) regulatory T cells is mediated by cell surface-bound transforming growth factor beta. The Journal of experimental medicine. 2001;194(5):629-44.

78. Peggs KS, Quezada SA, Chambers CA, Korman AJ, Allison JP. Blockade of CTLA-4 on both effector and regulatory T cell compartments contributes to the antitumor activity of anti-CTLA-4 antibodies. The Journal of experimental medicine. 2009;206(8):1717-25.

79. Wing K, Onishi Y, Prieto-Martin P, Yamaguchi T, Miyara M, Fehervari Z, et al. CTLA-4 control over Foxp3+ regulatory T cell function. Science (New York, NY). 2008;322(5899):271-5.

80. Pedroza-Gonzalez A, Verhoef C, Ijzermans JN, Peppelenbosch MP, Kwekkeboom J, Verheij J, et al. Activated tumor-infiltrating CD4+ regulatory T cells restrain antitumor immunity in patients with primary or metastatic liver cancer. Hepatology (Baltimore, Md). 2013;57(1):183-94.

81. Curiel TJ, Coukos G, Zou L, Alvarez X, Cheng P, Mottram P, et al. Specific recruitment of regulatory T cells in ovarian carcinoma fosters immune privilege and predicts reduced survival. Nat Med. 2004;10(9):942-9.

82. Gobert M, Treilleux I, Bendriss-Vermare N, Bachelot T, Goddard-Leon S, Arfi V, et al. Regulatory T cells recruited through CCL22/CCR4 are selectively activated in lymphoid infiltrates surrounding primary breast tumors and lead to an adverse clinical outcome. Cancer research. 2009;69(5):2000-9.

83. Kim S, Lee A, Lim W, Park S, Cho MS, Koo H, et al. Zonal difference and prognostic significance of foxp3 regulatory T cell infiltration in breast cancer. Journal of breast cancer. 2014;17(1):8-17.

84. Fu J, Xu D, Liu Z, Shi M, Zhao P, Fu B, et al. Increased regulatory T cells correlate with CD8 T-cell impairment and poor survival in hepatocellular carcinoma patients. Gastroenterology. 2007;132(7):2328-39.

85. Salama P, Phillips M, Grieu F, Morris M, Zeps N, Joseph D, et al. Tumor-infiltrating FOXP3+ T regulatory cells show strong prognostic significance in colorectal cancer. Journal of clinical oncology : official journal of the American Society of Clinical Oncology. 2009;27(2):186-92.

86. Golubovskaya V, Wu L. Different Subsets of T Cells, Memory, Effector Functions, and CAR-T Immunotherapy. Cancers (Basel). 2016;8(3).

87. Sallusto F, Geginat J, Lanzavecchia A. Central memory and effector memory T cell subsets: function, generation, and maintenance. Annual review of immunology. 2004;22:745-63.

88. Ahmadvand S, Faghih Z, Montazer M, Safaei A, Mokhtari M, Jafari P, et al. Importance of CD45RO+ tumor-infiltrating lymphocytes in post-operative survival of breast cancer patients. Cellular oncology (Dordrecht). 2019;42(3):343-56.

89. Galon J, Costes A, Sanchez-Cabo F, Kirilovsky A, Mlecnik B, Lagorce-Pages C, et al. Type, density, and location of immune cells within human colorectal tumors predict clinical outcome. Science (New York, NY). 2006;313(5795):1960-4.

90. Kong JC, Guerra GR, Pham T, Mitchell C, Lynch AC, Warrier SK, et al. Prognostic Impact of Tumor-Infiltrating Lymphocytes in Primary and Metastatic Colorectal Cancer: A Systematic Review and Meta-analysis. Diseases of the colon and rectum. 2019;62(4):498-508.

91. Lee HE, Chae SW, Lee YJ, Kim MA, Lee HS, Lee BL, et al. Prognostic implications of type and density of tumour-infiltrating lymphocytes in gastric cancer. British journal of cancer. 2008;99(10):1704-11.

92. Pages F, Berger A, Camus M, Sanchez-Cabo F, Costes A, Molidor R, et al. Effector memory T cells, early metastasis, and survival in colorectal cancer. The New England journal of medicine. 2005;353(25):2654-66.

93. Zhang Q, Lou Y, Yang J, Wang J, Feng J, Zhao Y, et al. Integrated multiomic analysis reveals comprehensive tumour heterogeneity and novel immunophenotypic classification in hepatocellular carcinomas. Gut. 2019;68(11):2019-31.

94. Yao Q, Bao X, Xue R, Liu H, Liu H, Li J, et al. Prognostic value of immunoscore to identify mortality outcomes in adults with HBV-related primary hepatocellular carcinoma. Medicine. 2017;96(17):e6735.

95. Suárez-Sánchez FJ, Lequerica-Fernández P, Rodrigo JP, Hermida-Prado F, Suárez-Canto J, Rodríguez-Santamarta T, et al. Tumor-Infiltrating CD20(+) B Lymphocytes:

Significance and Prognostic Implications in Oral Cancer Microenvironment. Cancers (Basel). 2021;13(3).

96. Pavlasova G, Mraz M. The regulation and function of CD20: an "enigma" of B-cell biology and targeted therapy. Haematologica. 2020;105(6):1494-506.

97. DeFalco J, Harbell M, Manning-Bog A, Baia G, Scholz A, Millare B, et al. Non-progressing cancer patients have persistent B cell responses expressing shared antibody paratopes that target public tumor antigens. Clinical immunology (Orlando, Fla). 2018;187:37-45.

98. Nussing S, Sant S, Koutsakos M, Subbarao K, Nguyen THO, Kedzierska K. Innate and adaptive T cells in influenza disease. Frontiers of medicine. 2018;12(1):34-47.

99. DiLillo DJ, Yanaba K, Tedder TF. B cells are required for optimal CD4+ and CD8+ T cell tumor immunity: therapeutic B cell depletion enhances B16 melanoma growth in mice. Journal of immunology (Baltimore, Md : 1950). 2010;184(7):4006-16.

100. Harris DP, Goodrich S, Gerth AJ, Peng SL, Lund FE. Regulation of IFN-gamma production by B effector 1 cells: essential roles for T-bet and the IFN-gamma receptor. Journal of immunology (Baltimore, Md : 1950). 2005;174(11):6781-90.

101. Lund FE, Randall TD. Effector and regulatory B cells: modulators of CD4+ T cell immunity. Nature reviews Immunology. 2010;10(4):236-47.

102. Wouters MCA, Nelson BH. Prognostic Significance of Tumor-Infiltrating B Cells and Plasma Cells in Human Cancer. Clin Cancer Res. 2018;24(24):6125-35.

103. Shi JY, Gao Q, Wang ZC, Zhou J, Wang XY, Min ZH, et al. Margin-infiltrating CD20(+) B cells display an atypical memory phenotype and correlate with favorable prognosis in hepatocellular carcinoma. Clin Cancer Res. 2013;19(21):5994-6005.

104. Miligy I, Mohan P, Gaber A, Aleskandarany MA, Nolan CC, Diez-Rodriguez M, et al. Prognostic significance of tumour infiltrating B lymphocytes in breast ductal carcinoma in situ. Histopathology. 2017;71(2):258-68.

105. Jiang Y, Li Y, Zhu B. T-cell exhaustion in the tumor microenvironment. Cell death & disease. 2015;6(6):e1792-e.

106. Wherry EJ, Kurachi M. Molecular and cellular insights into T cell exhaustion. Nat Rev Immunol. 2015;15(8):486-99.

107. Zhao X, Subramanian S. Intrinsic Resistance of Solid Tumors to Immune Checkpoint Blockade Therapy. Cancer research. 2017;77(4):817-22.

108. Nishimura H, Nose M, Hiai H, Minato N, Honjo T. Development of Lupus-like Autoimmune Diseases by Disruption of the PD-1 Gene Encoding an ITIM Motif-Carrying Immunoreceptor. Immunity. 1999;11(2):141-51.

109. Wherry EJ. T cell exhaustion. Nature immunology. 2011;12(6):492-9.

110. Bonorino C, Mognol G. Editorial: T Cell Exhaustion. Front Immunol. 2020;11:920.

111. Pico de Coaña Y, Choudhury A, Kiessling R. Checkpoint blockade for cancer therapy: revitalizing a suppressed immune system. Trends in molecular medicine. 2015;21(8):482-91.

112. Darvin P, Toor SM, Sasidharan Nair V, Elkord E. Immune checkpoint inhibitors: recent progress and potential biomarkers. Experimental & molecular medicine. 2018;50(12):1-11.

113. Dong H, Chen L. B7-H1 pathway and its role in the evasion of tumor immunity. Journal of molecular medicine (Berlin, Germany). 2003;81(5):281-7.

114. Dong H, Strome SE, Salomao DR, Tamura H, Hirano F, Flies DB, et al. Tumor-associated B7-H1 promotes T-cell apoptosis: a potential mechanism of immune evasion. Nat Med. 2002;8(8):793-800.

115. Mendes F, Domingues C, Rodrigues-Santos P, Abrantes AM, Goncalves AC, Estrela J, et al. The role of immune system exhaustion on cancer cell escape and anti-tumor immune induction after irradiation. Biochimica et biophysica acta. 2016;1865(2):168-75.

116. Haanen JB, Robert C. Immune Checkpoint Inhibitors. Progress in tumor research. 2015;42:55-66.

117. Ghebeh H, Mohammed S, Al-Omair A, Qattan A, Lehe C, Al-Qudaihi G, et al. The B7-H1 (PD-L1) T lymphocyte-inhibitory molecule is expressed in breast cancer patients with infiltrating ductal carcinoma: correlation with important high-risk prognostic factors. Neoplasia (New York, NY). 2006;8(3):190-8.

118. Curiel TJ, Wei S, Dong H, Alvarez X, Cheng P, Mottram P, et al. Blockade of B7-H1 improves myeloid dendritic cell-mediated antitumor immunity. Nat Med. 2003;9(5):562-7.

119. Zou W, Chen L. Inhibitory B7-family molecules in the tumour microenvironment. Nature reviews Immunology. 2008;8(6):467-77.

120. Xie Z, Chen Y, Zhao S, Yang Z, Yao X, Guo S, et al. Intrahepatic PD-1/PD-L1 up-regulation closely correlates with inflammation and virus replication in patients with chronic HBV infection. Immunological investigations. 2009;38(7):624-38.

121. Jiang Y, Li Y, Zhu B. T-cell exhaustion in the tumor microenvironment. Cell death & disease. 2015;6:e1792.

122. Zhang Y, Kang S, Shen J, He J, Jiang L, Wang W, et al. Prognostic Significance of Programmed Cell Death 1 (PD-1) or PD-1 Ligand 1 (PD-L1) Expression in Epithelial-Originated Cancer: A Meta-Analysis. 2015;94(6):e515.

123. Liu F, Liu Y, Chen Z. Tim-3 expression and its role in hepatocellular carcinoma. Journal of hematology & oncology. 2018;11(1):126.

124. Rangachari M, Zhu C, Sakuishi K, Xiao S, Karman J, Chen A, et al. Bat3 promotes T cell responses and autoimmunity by repressing Tim-3–mediated cell death and exhaustion. Nat Med. 2012;18(9):1394-400.

125. Cao Y, Zhou X, Huang X, Li Q, Gao L, Jiang L, et al. Tim-3 expression in cervical cancer promotes tumor metastasis. PloS one. 2013;8(1):e53834.

126. Komohara Y, Morita T, Annan DA, Horlad H, Ohnishi K, Yamada S, et al. The Coordinated Actions of TIM-3 on Cancer and Myeloid Cells in the Regulation of Tumorigenicity and Clinical Prognosis in Clear Cell Renal Cell Carcinomas. Cancer Immunol Res. 2015;3(9):999-1007.

127. Zhang Y, Cai P, Liang T, Wang L, Hu L. TIM-3 is a potential prognostic marker for patients with solid tumors: A systematic review and meta-analysis. Oncotarget. 2017;8(19):31705-13.

128. Ge W, Li J, Fan W, Xu D, Sun S. Tim-3 as a diagnostic and prognostic biomarker of osteosarcoma. Tumour biology : the journal of the International Society for Oncodevelopmental Biology and Medicine. 2017;39(7):1010428317715643.

129. Formenti SC, Demaria S. Systemic effects of local radiotherapy. The Lancet Oncology. 2009;10(7):718-26.

130. Galon J, Mlecnik B, Bindea G, Angell HK, Berger A, Lagorce C, et al. Towards the introduction of the 'Immunoscore' in the classification of malignant tumours. J Pathol. 2014;232(2):199-209.

131. Wang Y, Lin HC, Huang MY, Shao Q, Wang ZQ, Wang FH, et al. The Immunoscore system predicts prognosis after liver metastasectomy in colorectal cancer liver metastases. Cancer immunology, immunotherapy : CII. 2018;67(3):435-44.

132. Pages F, Mlecnik B, Marliot F, Bindea G, Ou FS, Bifulco C, et al. International validation of the consensus Immunoscore for the classification of colon cancer: a prognostic and accuracy study. Lancet. 2018;391(10135):2128-39.

133. Pagès F, Kirilovsky A, Mlecnik B, Asslaber M, Tosolini M, Bindea G, et al. In situ cytotoxic and memory T cells predict outcome in patients with early-stage colorectal cancer. Journal of clinical oncology : official journal of the American Society of Clinical Oncology. 2009;27(35):5944-51.

134. Peng J, Wang Y, Zhang R, Deng Y, Xiao B, Ou Q, et al. Immune Cell Infiltration in the Microenvironment of Liver Oligometastasis from Colorectal Cancer: Intratumoural CD8/CD3 Ratio Is a Valuable Prognostic Index for Patients Undergoing Liver Metastasectomy. Cancers (Basel). 2019;11(12).

135. Sideras K, Galjart B, Vasaturo A, Pedroza-Gonzalez A, Biermann K, Mancham S, et al. Prognostic value of intra-tumoral CD8(+) /FoxP3(+) lymphocyte ratio in patients with resected colorectal cancer liver metastasis. Journal of surgical oncology. 2018;118(1):68-76.

136. Shinto E, Hase K, Hashiguchi Y, Sekizawa A, Ueno H, Shikina A, et al. CD8+ and FOXP3+ tumor-infiltrating T cells before and after chemoradiotherapy for rectal cancer. Annals of surgical oncology. 2014;21 Suppl 3:S414-21.

137. Katz SC, Bamboat ZM, Maker AV, Shia J, Pillarisetty VG, Yopp AC, et al. Regulatory T cell infiltration predicts outcome following resection of colorectal cancer liver metastases. Annals of surgical oncology. 2013;20(3):946-55.

138. Schneider CA, Rasband WS, Eliceiri KW. NIH Image to ImageJ: 25 years of image analysis. Nature methods. 2012;9(7):671-5.

139. Eisenhauer EA, Therasse P, Bogaerts J, Schwartz LH, Sargent D, Ford R, et al. New response evaluation criteria in solid tumours: revised RECIST guideline (version 1.1). European journal of cancer (Oxford, England : 1990). 2009;45(2):228-47.

140. Wara WM. Immunosuppression associated with radiation therapy. Int J Radiat Oncol Biol Phys. 1977;2(5-6):593-6.

141. Walle T, Martinez Monge R, Cerwenka A, Ajona D, Melero I, Lecanda F. Radiation effects on antitumor immune responses: current perspectives and challenges. Ther Adv Med Oncol. 2018;10:1758834017742575.

142. de la Cruz-Merino L, Illescas-Vacas A, Grueso-López A, Barco-Sánchez A, Míguez-Sánchez C. Radiation for Awakening the Dormant Immune System, a Promising Challenge to be Explored. Front Immunol. 2014;5:102.

143. Vatner RE, Cooper BT, Vanpouille-Box C, Demaria S, Formenti SC. Combinations of immunotherapy and radiation in cancer therapy. Front Oncol. 2014;4:325.

144. Barsoum IB, Smallwood CA, Siemens DR, Graham CH. A mechanism of hypoxia-mediated escape from adaptive immunity in cancer cells. Cancer research. 2014;74(3):665-74.

145. Frey B, Ruckert M, Weber J, Mayr X, Derer A, Lotter M, et al. Hypofractionated Irradiation Has Immune Stimulatory Potential and Induces a Timely Restricted Infiltration of Immune Cells in Colon Cancer Tumors. Front Immunol. 2017;8:231.

146. Hettich M, Lahoti J, Prasad S, Niedermann G. Checkpoint Antibodies but not T Cell-Recruiting Diabodies Effectively Synergize with TIL-Inducing gamma-Irradiation. Cancer research. 2016;76(16):4673-83.

147. Chew V, Lee YH, Pan L, Nasir NJM, Lim CJ, Chua C, et al. Immune activation underlies a sustained clinical response to Yttrium-90 radioembolisation in hepatocellular carcinoma. Gut. 2019;68(2):335-46.

148. Mackall CL, Fleisher TA, Brown MR, Magrath IT, Shad AT, Horowitz ME, et al. Lymphocyte depletion during treatment with intensive chemotherapy for cancer. Blood. 1994;84(7):2221-8.

149. Verma R, Foster RE, Horgan K, Mounsey K, Nixon H, Smalle N, et al. Lymphocyte depletion and repopulation after chemotherapy for primary breast cancer. Breast Cancer Res. 2016;18(1):10.

150. Zhu Q, Cai MY, Weng DS, Zhao JJ, Pan QZ, Wang QJ, et al. PD-L1 expression patterns in tumour cells and their association with CD8(+) tumour infiltrating lymphocytes in clear cell renal cell carcinoma. Journal of Cancer. 2019;10(5):1154-61.

151. Jiang Y, Li Y, Zhu B. T-cell exhaustion in the tumor microenvironment. Cell death & disease. 2015;6(6):e1792.

152. Sun L, Zhang L, Yu J, Zhang Y, Pang X, Ma C, et al. Clinical efficacy and safety of anti-PD-1/PD-L1 inhibitors for the treatment of advanced or metastatic cancer: a systematic review and meta-analysis. Sci Rep. 2020;10(1):2083.

153. Li S, Sun S, Xiang H, Yang J, Peng M, Gao Q. Liver metastases and the efficacy of the PD-1 or PD-L1 inhibitors in cancer: a meta-analysis of randomized controlled trials. Oncoimmunology. 2020;9(1):1746113.

154. Wu J, Lin G, Zhu Y, Zhang H, Shi G, Shen Y, et al. Low TIM3 expression indicates poor prognosis of metastatic prostate cancer and acts as an independent predictor of castration resistant status. Sci Rep. 2017;7(1):8869.

155. Byun KD, Hwang HJ, Park KJ, Kim MC, Cho SH, Ju MH, et al. T-Cell Immunoglobulin Mucin 3 Expression on Tumor Infiltrating Lymphocytes as a Positive Prognosticator in Triple-Negative Breast Cancer. J Breast Cancer. 2018;21(4):406-14.

156. Zhou E, Huang Q, Wang J, Fang C, Yang L, Zhu M, et al. Up-regulation of Tim-3 is associated with poor prognosis of patients with colon cancer. Int J Clin Exp Pathol. 2015;8(7):8018-27.

157. Kato R, Jinnouchi N, Tuyukubo T, Ikarashi D, Matsuura T, Maekawa S, et al. TIM3 expression on tumor cells predicts response to anti-PD-1 therapy for renal cancer. Transl Oncol. 2021;14(1):100918.

158. Zhang X, Yin X, Zhang H, Sun G, Yang Y, Chen J, et al. Differential expression of TIM-3 between primary and metastatic sites in renal cell carcinoma. BMC Cancer. 2019;19(1):49.

159. Li Z, Li N, Li F, Zhou Z, Sang J, Chen Y, et al. Immune checkpoint proteins PD-1 and TIM-3 are both highly expressed in liver tissues and correlate with their gene polymorphisms in patients with HBV-related hepatocellular carcinoma. Medicine (Baltimore). 2016;95(52):e5749.

160. Qin S, Dong B, Yi M, Chu Q, Wu K. Prognostic Values of TIM-3 Expression in Patients With Solid Tumors: A Meta-Analysis and Database Evaluation. Front Oncol. 2020;10:1288.

161. Chao X, Liu L, Sun P, Yang X, Li M, Luo R, et al. Immune parameters associated with survival in metaplastic breast cancer. Breast cancer research : BCR. 2020;22(1):92.

162. Stenzel PJ, Schindeldecker M, Tagscherer KE, Foersch S, Herpel E, Hohenfellner M, et al. Prognostic and Predictive Value of Tumor-infiltrating Leukocytes and of Immune Checkpoint Molecules PD1 and PDL1 in Clear Cell Renal Cell Carcinoma. Translational oncology. 2020;13(2):336-45.

163. Li Y, Liang L, Dai W, Cai G, Xu Y, Li X, et al. Prognostic impact of programed cell death-1 (PD-1) and PD-ligand 1 (PD-L1) expression in cancer cells and tumor infiltrating lymphocytes in colorectal cancer. Molecular cancer. 2016;15(1):55.

164. Kahlmeyer A, Stöhr CG, Hartmann A, Goebell PJ, Wullich B, Wach S, et al. Expression of PD-1 and CTLA-4 Are Negative Prognostic Markers in Renal Cell Carcinoma. Journal of clinical medicine. 2019;8(5).

165. Lee LH, Cavalcanti MS, Segal NH, Hechtman JF, Weiser MR, Smith JJ, et al. Patterns and prognostic relevance of PD-1 and PD-L1 expression in colorectal carcinoma. Modern Pathology. 2016;29(11):1433-42.

166. Zhou SN, Pan WT, Pan MX, Luo QY, Zhang L, Lin JZ, et al. Comparison of Immune Microenvironment Between Colon and Liver Metastatic Tissue in Colon Cancer Patients with Liver Metastasis. Dig Dis Sci. 2021;66(2):474-82.

167. Sobottka B, Pestalozzi B, Fink D, Moch H, Varga Z. Similar lymphocytic infiltration pattern in primary breast cancer and their corresponding distant metastases. Oncoimmunology. 2016;5(6):e1153208.

168. Hou J, Zhang H, Sun B, Karin M. The immunobiology of hepatocellular carcinoma in humans and mice: Basic concepts and therapeutic implications. Journal of hepatology. 2020;72(1):167-82.

169. Schreiber RD, Old LJ, Smyth MJ. Cancer immunoediting: integrating immunity's roles in cancer suppression and promotion. Science. 2011;331(6024):1565-70.

170. Edin S, Kaprio T, Hagstrom J, Larsson P, Mustonen H, Bockelman C, et al. The Prognostic Importance of CD20(+) B lymphocytes in Colorectal Cancer and the Relation to Other Immune Cell subsets. Sci Rep. 2019;9(1):19997.

171. Porcellato I, Silvestri S, Menchetti L, Recupero F, Mechelli L, Sforna M, et al. Tumour-infiltrating lymphocytes in canine melanocytic tumours: An investigation on the prognostic role of CD3(+) and CD20(+) lymphocytic populations. Vet Comp Oncol. 2020;18(3):370-80.

172. Sarvaria A, Madrigal JA, Saudemont A. B cell regulation in cancer and anti-tumor immunity. Cellular & molecular immunology. 2017;14(8):662-74.

173. Peng B, Ming Y, Yang C. Regulatory B cells: the cutting edge of immune tolerance in kidney transplantation. Cell Death Dis. 2018;9(2):109.

174. Chong AS, Khiew SH. Transplantation tolerance: don't forget about the B cells. Clin Exp Immunol. 2017;189(2):171-80.

175. Mlecnik B, Van den Eynde M, Bindea G, Church SE, Vasaturo A, Fredriksen T, et al. Comprehensive Intrametastatic Immune Quantification and Major Impact of Immunoscore on Survival. J Natl Cancer Inst. 2018;110(1).

176. Guo M, Yuan F, Qi F, Sun J, Rao Q, Zhao Z, et al. Expression and clinical significance of LAG-3, FGL1, PD-L1 and CD8(+)T cells in hepatocellular carcinoma using multiplex quantitative analysis. Journal of translational medicine. 2020;18(1):306.

177. Kuwahara T, Hazama S, Suzuki N, Yoshida S, Tomochika S, Nakagami Y, et al. Intratumoural-infiltrating CD4 + and FOXP3 + T cells as strong positive predictive markers for the prognosis of resectable colorectal cancer. British journal of cancer. 2019;121(8):659-65.

178. Zhang Q, Hao C, Cheng G, Wang L, Wang X, Li C, et al. High CD4$^+$ T cell density is associated with poor prognosis in patients with non-muscle-invasive bladder cancer. International journal of clinical and experimental pathology. 2015;8(9):11510-6.

179. Hu G, Wang S. Tumor-infiltrating CD45RO(+) Memory T Lymphocytes Predict Favorable Clinical Outcome in Solid Tumors. Sci Rep. 2017;7(1):10376.

180. Blankenstein T, Coulie PG, Gilboa E, Jaffee EM. The determinants of tumour immunogenicity. Nature reviews Cancer. 2012;12(4):307-13.

181. Tagliamonte M, Mauriello A, Cavalluzzo B, Ragone C, Manolio C, Petrizzo A, et al. Tackling hepatocellular carcinoma with individual or combinatorial immunotherapy approaches. Cancer Lett. 2020;473:25-32.

182. Buonaguro L, Mauriello A, Cavalluzzo B, Petrizzo A, Tagliamonte M. Immunotherapy in hepatocellular carcinoma. Annals of hepatology. 2019;18(2):291-7.

183. Powerski M, Drewes R, Omari J, Relja B, Surov A, Pech M. Intra-hepatic Abscopal Effect Following Radioembolization of Hepatic Metastases. Cardiovascular and interventional radiology. 2020;43(11):1641-9.

184. Liu Y, Dong Y, Kong L, Shi F, Zhu H, Yu J. Abscopal effect of radiotherapy combined with immune checkpoint inhibitors. Journal of hematology & oncology. 2018;11(1):104.

185. Golden EB, Chhabra A, Chachoua A, Adams S, Donach M, Fenton-Kerimian M, et al. Local radiotherapy and granulocyte-macrophage colony-stimulating factor to generate abscopal responses in patients with metastatic solid tumours: a proof-of-principle trial. The Lancet Oncology. 2015;16(7):795-803.

9. Acknowledgements

I would like to thank Prof. Dr. med. Jens Ricke for offering me this wonderful opportunity to join the Department of Radiology where I conducted my research. I am very grateful for his kindness and great help throughout this project.

I would like to give my thanks to my Doctor father Prof. Dr. med. Clemens Cyran for his guidance and advice on my research project. I am extremely thankful for his generosity and willingness to help me at any moment.

I would like to also thank Dr. Marianna Alunni-Fabbroni for always giving me support in every shape, way and form. She is always patient and ready to help whenever I needed. She is an excellent supervisor in each phase of my work. This project could not have been realized without her.

I also owe big thanks to Prof. Dr. med. Martina Rudelius and Mr. Guido Piontek for their technical support and friendly cooperation on my project.

I would like to thank Dr. Heidrun Hirner-Eppeneder for reading the manuscript and making corrections. Also, a special thanks to Ms. Cheryl Gray for proofreading my thesis and being a good friend. In particular, I would like to thank our lab team for creating a lovely atmosphere where I enjoyed every minute of my study.

I also owe my deepest gratitude to my parents, Junqiang Gu and Wenjue Zhang from China for continuous moral support and encouragement over all these years.

Finally, I would like to thank everyone who has been helping me throughout my life. Nothing could have been achieved without them.

Eidesstattliche Versicherung

Ich, Sijing Gu, erkläre hiermit an Eides statt, dass ich die vorliegende Dissertation mit dem Thema

„Tumor-infiltrating lymphocytes as biomarkers to monitor local ablation of primary and secondary liver cancer ”

selbständig verfasst, mich außer der angegebenen keiner weiteren Hilfsmittel bedient und alle Erkenntnisse, die aus dem Schrifttum ganz oder annähernd übernommen sind, als solche kenntlich gemacht und nach ihrer Herkunft unter Bezeichnung der Fundstelle einzeln nachgewiesen habe.

Ich erkläre des Weiteren, dass die hier vorgelegte Dissertation nicht in gleicher oder in ähnlicher Form bei einer anderen Stelle zur Erlangung eines akademischen Grades eingereicht wurde.

München, 04.03.2023	**Sijing Gu**
Ort, Datum	Unterschrift Doktorandin